

NONINVASIVE TEMPERATURE ESTIMATION FOR HYPERTHERMIA USING PULSED ULTRASOUND

A dissertation
submitted in partial fulfillment of the requirements for
the degree of
Master of Technology

by

Jaydeep A. Gore

(Roll No. 00307406)

under the guidance of

Prof. T. Anjaneyulu

Prof. P. C. Pandey



Department of Electrical Engineering
Indian Institute of Technology, Bombay
Powai, Mumbai 400 076

January 2002

Acknowledgement

I would like to express my gratitude to my guides Prof. T. Anjaneyulu, and Prof. P.C. Pandey for their valuable guidance, support and encouragement throughout the course of this project.

I am indebted to Prof. C.P. Gadgil for providing background information, support and encouragement, and data from his earlier experiments.

I am thankful to my colleagues Ashwin Athram, Suhas Solanki, Anand Mirji and Tanmay Pawar for their help during the course of this project.

I would also like to thank Mr. Muntode of our Laboratory for his help.

Jaydeep Gore

January 2002

Jaydeep A. Gore/ Prof. T. Anjaneyulu and Prof. P.C. Pandey (guides):

”Noninvasive estimation of temperature for hyperthermia using pulsed ultrasound,” *M. Tech. dissertation*, Dept. of Electrical Engineering, Indian Institute of Technology, Bombay, January 2002.

Abstract

Hyperthermia is the application of heat to target tissues, as a cancer treatment therapy. For its effectiveness, noninvasive monitoring of the tissue temperature is needed. Reported techniques for measurement of temperature using ultrasound use a number of transducers and involved signal processing. In this project, use of a single piezoelectric transducer for noninvasively estimating temperature of a particular layer in a medium using pulsed ultrasound is investigated. The transfer function of the layer is computed from the spectra of the echoes, from the front and the back interface of the layer, received by the transducer. Parameters obtained from the magnitude and the phase part of the transfer function are investigated with an objective to identify parameters that could be used to develop an instrumentation system for monitoring temperature noninvasively.

Contents

Acknowledgement	i
Abstract	ii
List of figures	iv
List of tables	viii
List of symbols	ix
List of abbreviations	xi
1 Introduction	1
1.1 Problem overview	1
1.2 Scope of present work	2
1.3 Report outline	3
2 Ultrasound parameters for noninvasive temperature estimation	4
2.1 Introduction	4
2.2 Acoustic parameters	5
2.2.1 Acoustic velocity	5
2.2.2 Attenuation coefficient	5
2.2.3 Characteristic impedance	6
2.2.4 Transfer function	6
2.3 Estimation of transfer function	7
2.4 Investigations reported earlier	10

2.5	Estimation of attenuation coefficient from transfer function	12
2.6	Estimation of temperature from attenuation coefficient	18
3	Investigations in ultrasound thermometry with a single transducer	20
3.1	Introduction	20
3.2	Estimation of temperature from phase part of the transfer function	21
3.3	Estimation of temperature from magnitude part of the echo transfer function	22
3.4	Experimental setup	23
3.5	Signal processing	24
4	Results and discussions	28
4.1	Results	28
4.2	Transfer function energy ratio method	28
4.3	Phase response method	29
4.4	Mean squared transfer function	30
4.5	Discussions	30
5	Summary and conclusions	51
	References	53

List of Figures

2.1	Echoes in a multilayer system	9
2.2	(a) Sensitivity characteristics of transducers A, B, C, D. (b) Combined truncated magnitude division characteristics [3]	13
2.3	Effect of temperature on echo transfer function of Perspex and PVC [3] . . .	14
2.4	Use of weighting function for computation of attenuation coefficient	16
3.1	Experimental setup	24
3.2	The signal received by the transducer and the two gated echoes	27
4.1	Dependence of phase response of transfer function vs temperature. Perspex layer of 20 mm thickness. Transducer 2.5 MHz	33
4.2	Dependence of magnitude response vs temperature. Perspex layer of 20 mm thickness . Transducer 2.5 MHz	34
4.3	E_{R1} versus temperature θ for Water/Perspex/Water sample	35
4.4	E_{R1} versus temperature θ for Water/Perspex/Water sample	35
4.5	E_{R1} versus temperature θ for Water/PVC/Water/Perspex/air sample	36
4.6	F_ϕ versus temperature θ for a water/Perspex/water sample [Table 4.1, sample 1-3]	37
4.7	$S_{F\phi}(\theta)$ versus temperature θ for a water/Perspex/water sample [Table 4.1, sample 1-3]	37
4.8	F_ϕ versus temperature θ for a water/Perspex/water sample [Table 4.1, sample 4-5]	38
4.9	$S_{F\phi}(\theta)$ versus temperature θ for a water/Perspex/water sample [Table 4.2, sample 4-5]	38

4.10	F_ϕ versus temperature θ for a multilayered water/PVC/water/Perspex/air sample [Table 4.1, sample 6]	39
4.11	$S_{F_\phi}(\theta)$ versus temperature θ for a multilayered water/PVC/water/Perspex/air sample [Table 4.1, sample 6]	39
4.12	F_ϕ versus temperature θ for a multilayered water/Perspex/water/PVC/air sample [Table 4.1, sample 7]	40
4.13	$S_{F_\phi}(\theta)$ versus temperature θ for a multilayered water/Perspex/water/PVC/air sample [Table 4.1, sample 7]	40
4.14	F_ϕ versus temperature θ for a water/PVC/water sample [Table 4.2, sample 1-2]	41
4.15	$S_{F_\phi}(\theta)$ versus temperature θ for a water/PVC/water sample [Table 4.2, sample 1-2]	41
4.16	F_ϕ versus temperature θ for a multilayered water/PVC/water/Perspex/air sample [Table 4.2, sample 3]	42
4.17	$S_{F_\phi}(\theta)$ versus temperature θ for a multilayered water/PVC/water/Perspex/air sample [Table 4.2, sample 3]	42
4.18	F_ϕ versus temperature θ for a multilayered water/Perspex/water/PVC/air sample [Table 4.2, sample 4]	43
4.19	$S_{F_\phi}(\theta)$ versus temperature θ for a multilayered water/Perspex/water/PVC/air sample [Table 4.2, sample 4]	43
4.20	$ H_{avg}^2(\theta) $ versus temperature θ for a water/Perspex/water sample [Table 4.1, sample 1-3]	44
4.21	$S_{H^2_{avg}}(\theta)$ versus temperature θ for a water/Perspex/water sample [Table 4.1, sample 1-3]	44
4.22	$ H_{avg}^2(\theta) $ versus temperature θ for a water/Perspex/water sample [Table 4.1, sample 4-5]	45
4.23	$S_{H^2_{avg}}(\theta)$ versus temperature θ for a water/Perspex/water sample [Table 4.1, sample 4-5]	45
4.24	$ H_{avg}^2(\theta) $ versus temperature θ for a multilayered water/PVC/water/Perspex/air sample [Table 4.1, sample 6]	46

4.25	$S_{H^2_{avg}}(\theta)$ versus temperature θ for a multilayered water/PVC/water/ Perspex/air sample [Table 4.1, sample 6]	46
4.26	$ H^2_{avg}(\theta) $ versus temperature θ for a multilayered water/Perspex/water/ PVC/air sample [Table 4.1, sample 7]	47
4.27	$S_{H^2_{avg}}(\theta)$ versus temperature θ for a multilayered water/Perspex/water/ PVC/air sample [Table 4.1, sample 7]	47
4.28	$ H^2_{avg}(\theta) $ versus temperature θ for a water/PVC/water sample [Table 4.2, sample 1-2]	48
4.29	$S_{H^2_{avg}}(\theta)$ versus temperature θ for a water/PVC/water sample [Table 4.2, sample 1-2]	48
4.30	$ H^2_{avg}(\theta) $ versus temperature θ for a multilayered water/PVC/water/ Perspex/air sample [Table 4.2, sample 3]	49
4.31	$S_{H^2_{avg}}(\theta)$ versus temperature θ for a multilayered water/PVC/water/ Perspex/air sample [Table 4.2, sample 3]	49
4.32	$ H^2_{avg}(\theta) $ versus temperature θ for a multilayered water/Perspex/water/ PVC/air sample [Table 4.2, sample 4]	50
4.33	$S_{H^2_{avg}}(\theta)$ versus temperature θ for a multilayered water/Perspex/water/ PVC/air sample [Table 4.2, sample 4]	50

List of tables

2.1	Attenuation coefficient for Perspex and PVC using different methods as a function of temperature.....	18
2.2	Slope of relative change in attenuation coefficient.....	19
4.1	Slope of relative changes in F_ϕ and H^2avg for different layers/thicknesses/transducers/experimental setup (layer of interest - Perspex).....	31
4.2	Slope of relative changes in F_ϕ and H^2avg for different layers/thicknesses/transducers/experimental setup (layer of interest - PVC).....	31

List of symbols

c	velocity of ultrasound wave in a material
K	bulk modulus
ρ	density of the material
P_z	pressure of a plane ultrasonic wave propagating in the z direction
P_{zo}	pressure of a plane ultrasonic wave propagating in the z direction at $z = 0$
α	ultrasonic pressure wave attenuation coefficient
F	frequency of a signal wave
θ	temperature of a material
$\Delta\theta$	change in temperature
K_α	temperature variation constant for the attenuation coefficient of the layer
Z	acoustic characteristic impedance of a material
u_z	particle velocity in a material in the z direction
r	reflection coefficient of a material
Z_{cm}	acoustic characteristic impedance of coupling medium
$H_{rx}(F)$	transfer function of a piezoelectric transducer in the receiving mode
$H_{cm}(F)$	transfer function of the coupling medium
$H_{lut}(F)$	transfer function of a layer under test for transmission of signals through it
$H_{ol}(F)$	transfer function of the other layer
α	ultrasonic pressure wave attenuation coefficient
$p_o(t)$	acoustic pulse leaving the transducer surface
$p_1(t)$	reflected acoustic pulse(echo 1) from the front interface
$P_1(F)$	Fourier transform of $p_1(t)$
$P_2(F)$	Fourier transform of $p_2(t)$

$V_1(F)$	Fourier transform of transduced electrical signal corresponding to $P_1(F)$
$V_2(F)$	Fourier transform of transduced electrical signal corresponding to $P_2(F)$
$H_{2,1}(F)$	system transfer function of 2^{nd} layer
α_N	attenuation coefficient of N^{th} layer in dB/cm
c_N	velocity of ultrasound wave in N^{th} layer
$H_{N,N-1}$	system transfer function of N^{th} layer
D_F	rms bandwidth of a layer
F_m	suitable reference frequency at which the transfer function $ H(F) $ is maximum
a_N	attenuation coefficient of N^{th} layer in dB/(MHz-cm)
L_N	thickness of N^{th} layer
r_N	reflection coefficient at the N^{th} interface
$X(F)$	weighting function
E_1	weighted energy of $H_{N,N-1}(F)$ in the frequency band centered around frequency F_1
E_2	weighted energy of $H_{N,N-1}(F)$ in the frequency band centered around frequency F_2
$h_{N,N-1}(t)$	impulse response of N^{th} layer
t_c	instant of time at which a maximum of the layer impulse response occurs
t_1	instant of time where the magnitude of the layer impulse response is half its maximum
t_2	instant of time where the magnitude of the layer impulse response is half its maximum
D_t	rms time duration
ϕ	phase shift at frequency F
F_ϕ	frequency at which a phase shift of π radians occurs
$c_{\theta 0}$	acoustic velocity at temperature $\theta 0$
$c_{\theta 1}$	acoustic velocity at temperature $\theta 1$
K_c	temperature coefficient of acoustic velocity
$F_\phi(\theta 0)$	frequency at which a phase shift of π radians occurs at temperature $\theta 0$
$F_\phi(\theta 1)$	frequency at which a phase shift of π radians occurs at temperature $\theta 1$
$L_{\theta 0}$	thickness of layer of interest at temperature $\theta 0$
$L_{\theta 1}$	thickness of layer of interest at temperature $\theta 1$
$S_{F_\phi}(\theta)$	relative change in $F_\phi(\theta)$
$ H^2 avg(\theta) $	magnitude of mean squared pulse echo transfer function at temperature θ

$ H_{\theta}^2(F) $	magnitude squared of system transfer function of a layer at temperature θ
$S_{H^2avg(\theta)}$	relative change in $H^2avg(\theta)$

List of abbreviations

cm	coupling medium
lut	layer under test
ol	other layer

Chapter 1

Introduction

1.1 Problem overview

Hyperthermia is the application of heat to solid cancerous tissues. The effectiveness of established treatment therapies like radiation and chemotherapy increases with hyperthermia. In cancer therapy based on hyperthermia, the tumor temperature is elevated to a temperature of about 5 °C above the normal. This temperature is maintained for 30 min to 1 hour [8]. Thus there is a need for temperature monitoring of the cancerous tissue to ensure effective treatment. Most of the standard techniques for measuring temperature for hyperthermia use sensors that are invasive in nature. When used in an ultrasound therapy system, the sensors can act as ultrasound scatterers, and thus distort the ultrasound beam profile. Thus there is a need for monitoring temperature noninvasively. Ultrasound can be one such noninvasive technique.

Temperature affects acoustic properties of many materials like velocity, characteristic impedance, attenuation coefficient, etc. In ultrasound technique, ultrasonic energy in the form of pulses is incident on the medium of interest. The resulting back echo waveform is processed to estimate the change in the above mentioned acoustic properties, and changes in them may provide a measure of temperature.

Techniques based on changes in the acoustic velocity use the time of flight method for measurement of acoustic velocity. These techniques involve measurement of time of arrival of the reflected pulses. The change in the time of arrival with temperature is small as compared

to the times of arrival of the reflected echoes. Techniques for measurement of attenuation coefficient have been developed [4], [5]. These techniques are based on modeling the medium of interest as a linear time invariant system and computing its transfer function. Work carried out at IIT Bombay by Prof. C.P. Gadgil [3] concentrated on the estimation of acoustic velocity, layer impulse response, and parameters obtained from the impulse response. It concluded that attenuation coefficient is a potential parameter for monitoring temperature noninvasively. It has been shown that parameters obtained are independent of transducer properties. Due to the presence of measurement noise, a large number of narrow band transducers were used to improve the signal - to - noise ratio. Due to the use of a number of narrow band transducers and involved signal processing, this method cannot be easily adapted for developing an instrumentation system for estimating temperature.

This project investigates the use of a single ultrasonic piezoelectric transducer for estimating the temperature of a material noninvasively. Parameters obtained from the magnitude and the phase parts of the transfer function computed within the region of confidence of the transducer are investigated to find if reliable estimates of temperature can be obtained from them.

1.2 Scope of present work

The objective is to identify parameters that can be used for developing an instrument for monitoring temperature of medium of interest noninvasively. The material of interest is modeled as a linear time invariant system. The material can then be completely characterized in the frequency domain by its transfer function. The work aims to study the changes in the spectrum of the pulse echo waveform as a function of temperature.

In addition to attenuation through the tissue layer, interface reflections are also likely to be sensitive to temperature. Data acquired by Gadgil [3] in his experiments using pulsed ultrasound was analyzed. In experiments with Perspex and polyvinylchloride, it is seen that the temperature sensitivity of the magnitude of the transfer function is comparatively more in the region of confidence of the transducer used to transmit and receive ultrasound signals. The magnitude and the phase responses of the transfer function at different test temperatures

are studied to identify suitable parameters which can be used in an instrumentation system to estimate the temperature of the material, noninvasively.

Perspex, an amorphous material with acoustic properties comparable to that of biological tissues is used as a test medium. Keeping in view the applicability in the clinical field, the range of temperature variation - room temperature to about $50^{\circ}C$ - has been studied. Experiments were carried out with Perspex sheet of different thicknesses. Data related to experiments carried out by Gadgil [3] on multilayered media consisting of Perspex and polyvinylchloride were also analyzed.

1.3 Report outline

The following chapter reviews literature on acoustic parameter estimation for temperature measurement. A very brief overview of the work carried out by Gadgil [3] is discussed in the same chapter. The measurement setup, data acquisition procedure, and analysis of experimental data are discussed in Chapter 3. Results obtained and discussions are included in Chapter 4. Summary and conclusions, and suggestions for future work are presented in the last chapter.

Chapter 2

Ultrasound parameters for noninvasive temperature estimation

2.1 Introduction

Ultrasound is preferred as a means for measuring temperature because it has good directivity and is easy to generate and safe to handle. Further, information in the form of amplitude and phase relationships amongst the reflected pulses from the interfaces of multilayered materials can be easily acquired. It has no hazards of ionizing radiations at low intensities. The only limitation of ultrasound is its inability to propagate through vacuum or air.

Temperature of a material is usually measured by:

1. Introducing a sensor of known temperature-dependent physical properties.
2. Measuring the temperature dependent properties of the medium.

In a multilayered tissue where the layer of interest is inaccessible, the only alternative is to rely on the tissue as its own sensor. Acoustic propagation is affected when materials under test are exposed to temperature changes. An ultrasonic signal is sent into the material and the reflected or transmitted signals from the layer of interest are acquired and analyzed to extract information on potential parameters that can be used for measuring temperature. These parameters could be acoustic velocity, attenuation coefficient, characteristic

impedance, and related nonphysical parameters like layer transfer function, layer impulse response etc. A brief introduction to these parameters is given in the following sections.

Section 2.2 in this chapter presents a brief overview of acoustic parameters. Section 2.3 briefly reviews the work carried out by Gadgil [3]. This section discusses various acoustic parameter estimation techniques, signal processing issues, and limitations of these techniques.

2.2 Acoustic parameters

This section gives a brief overview of acoustic parameters that could provide a measure of temperature.

2.2.1 Acoustic velocity

The velocity c of ultrasound wave, in a material is given by [9]

$$c = \left(\frac{K}{\rho}\right)^{1/2} \quad (2.1)$$

where K = the bulk modulus, ρ = density of the material. Acoustic velocity is a function of temperature as both the bulk modulus K and the density ρ are a function of temperature. Velocity can be measured using pulse echo techniques. It can be calculated by measuring the time of flight of the reflected ultrasound pulses or can also can be estimated from the transfer function of the material.

2.2.2 Attenuation coefficient

When an ultrasonic wave propagates through a material, its energy is reduced as a function of distance. The energy may be diverted by reflection and scattering, or may be absorbed by the tissue and converted to heat. The pressure P_z of a plane wave propagating in the z direction at a distance z can be expressed as:

$$P_z = P_{zo}e^{-\alpha z} \quad (2.2)$$

where P_{zo} is the pressure at $z = 0$, and α is the pressure wave attenuation coefficient.

Attenuation coefficient is a function of frequency (F), and temperature (θ). Assuming that the changes in the length of the material with temperature are small enough to be neglected, it is possible to estimate changes in the temperature by estimating the attenuation coefficient. If the temperature ranges are small, attenuation can be considered to vary linearly with temperature,

$$\alpha_{\theta+\Delta\theta} = \alpha_{\theta}(1 + k_{\alpha}\Delta\theta) \quad (2.3)$$

where k_{α} is the temperature variation constant for the attenuation coefficient of the layer.

2.2.3 Characteristic impedance

Characteristic impedance (Z) of a material is the ratio of pressure of the ultrasonic wave to the particle velocity in the material [9] and is given as

$$Z = \frac{P_z}{u_z} = \rho c \quad (2.4)$$

where, P_z is the ultrasonic wave pressure in the direction of travel, u_z is the particle velocity in the same direction.

Characteristic impedance is a function of temperature as density ρ of the medium and acoustic velocity c vary with temperature. Characteristic impedance can be calculated from the reflection coefficient, r , of the medium using the equation :

$$r = \frac{Z - Z_{cm}}{Z + Z_{cm}} \quad (2.5)$$

Z_{cm} is the characteristic impedance of the coupling medium.

2.2.4 Transfer function

The material under test is modelled as a linear time invariant system which can be characterized by its transfer function in the frequency domain. The reflected ultrasound echoes are received by a piezoelectric transducer and the resulting signals are processed in the frequency domain to obtain the transfer function. For a set-up consisting of n layers, the transfer function of a layer is defined as the ratio of the Fourier transform of the received echoes from the rear and front interfaces of the layer.

Transfer function is related to physical properties of the medium like acoustic velocity, attenuation coefficient, reflection coefficient, etc. and hence varies with temperature. The transfer function can be used for estimation of one or more of these parameters, which in turn can be used for temperature estimation. The transfer function may itself also be used as a temperature estimator.

2.3 Estimation of transfer function

Ultrasound signals of various types, namely continuous, sine-burst, and pulsed are used for estimating acoustic parameters of materials.

To characterize a material, its response to a known input has to be studied. The input to the system and its response are measured using a pair of transducers in a transmission type system. In such cases the transducer transfer function has to be considered along with the system transfer function. Further, for an inaccessible layer, the effect of all the layers has to be considered. This poses a severe difficulty because the transfer function of other layers are also temperature dependent.

In a system using pulse echo technique, a reflection from the first interface corresponding to the input signal and a reflection from the second interface corresponding to the response are received by the same transducer from the layer of interest. It has been shown below that the ratio of the two reflected signals becomes independent of the transducer transfer function. Acoustic parameters like attenuation coefficient, velocity, and characteristic impedance can be measured from the ratio of the two reflected signals [3]

The system model of the echo generation process is shown in Fig 2.1. Let,

$H_{rx}(F)$ = the transfer function of the transducer in the receiving mode.

$H_{cm}(F)$ = the transfer function of the coupling medium.

$H_{lut}(F)$ = the transfer function of the layer under test, for transmission of signals through it.

$H_{ol}(F)$ = the transfer function of the other layer.

$p_o(t)$ = the acoustic pulse leaving the transducer surface.

$p_1(t)$ = the reflected pulse (echo1) from the front.

$p_2(t)$ = the reflected pulse (echo2) from the back.

Pulse $p_o(t)$ travels in the coupling medium toward the front interface. A part of this pulse gets reflected at the first interface and a part gets transmitted into the layer under test. The reflected pulse is $p_1(t)$ and the transmitted pulse is $p_{1z}(t)$, which travels in the layer under test and gets partially reflected at the back interface. It travels towards the first interface and it comes out of the layer as $p_2(t)$ as a partially transmitted signal representing the response of the layer under test to the excitation. Both the echoes $p_1(t)$ and $p_2(t)$ are transduced as electrical signals. The two echoes are characterized in the frequency domain by the following equations :

$$P_1(F) = r_1 P_0(F) H_{cm}(F) \quad (2.6)$$

$$P_2(F) = P_0(F) H_{cm}(F) (1 - r_1) H_{lut}(F) r_2 H_{lut}(F) (1 - r_1) H_{cm}(F) \quad (2.7)$$

where r_1 and r_2 are the reflection coefficients at the front and back interfaces respectively. If $V_1(F)$ and $V_2(F)$ are Fourier transforms of the transduced electrical signals, then,

$$V_1(F) = H_{rx}(F) P_1(F) \quad (2.8)$$

$$V_2(F) = H_{rx}(F) P_2(F) \quad (2.9)$$

The system transfer function can be obtained by :

$$H_{2,1}(F) = \frac{V_2(F)}{V_1(F)} = \frac{H_{rx}(F) P_2(F)}{H_{rx}(F) P_1(F)} \quad (2.10)$$

From Eqn 2.8, 2.9 and 2.10

$$\begin{aligned} H_{2,1}(F) &= \frac{P_o(F) H_{cm}^2(F) (1 - r_1)^2 H_{lut}^2(F) r_2}{P_o(F) H_{cm}^2(F) r_1} \\ &= \frac{(1 - r_1^2) r_2}{r_1} H_{lut}^2(F) \end{aligned} \quad (2.11)$$

Thus the transfer function obtained is independent of the transfer functions of the transducer and the coupling medium. The layer transfer function is a function of the attenuation coefficient α of the layer, acoustic velocity c of the ultrasonic wave in the medium, and the layer thickness L . The layer transfer function can be given as :

$$H_{lut}(F) = e^{-\alpha(F)L} e^{-j2\pi FL/c} \quad (2.12)$$

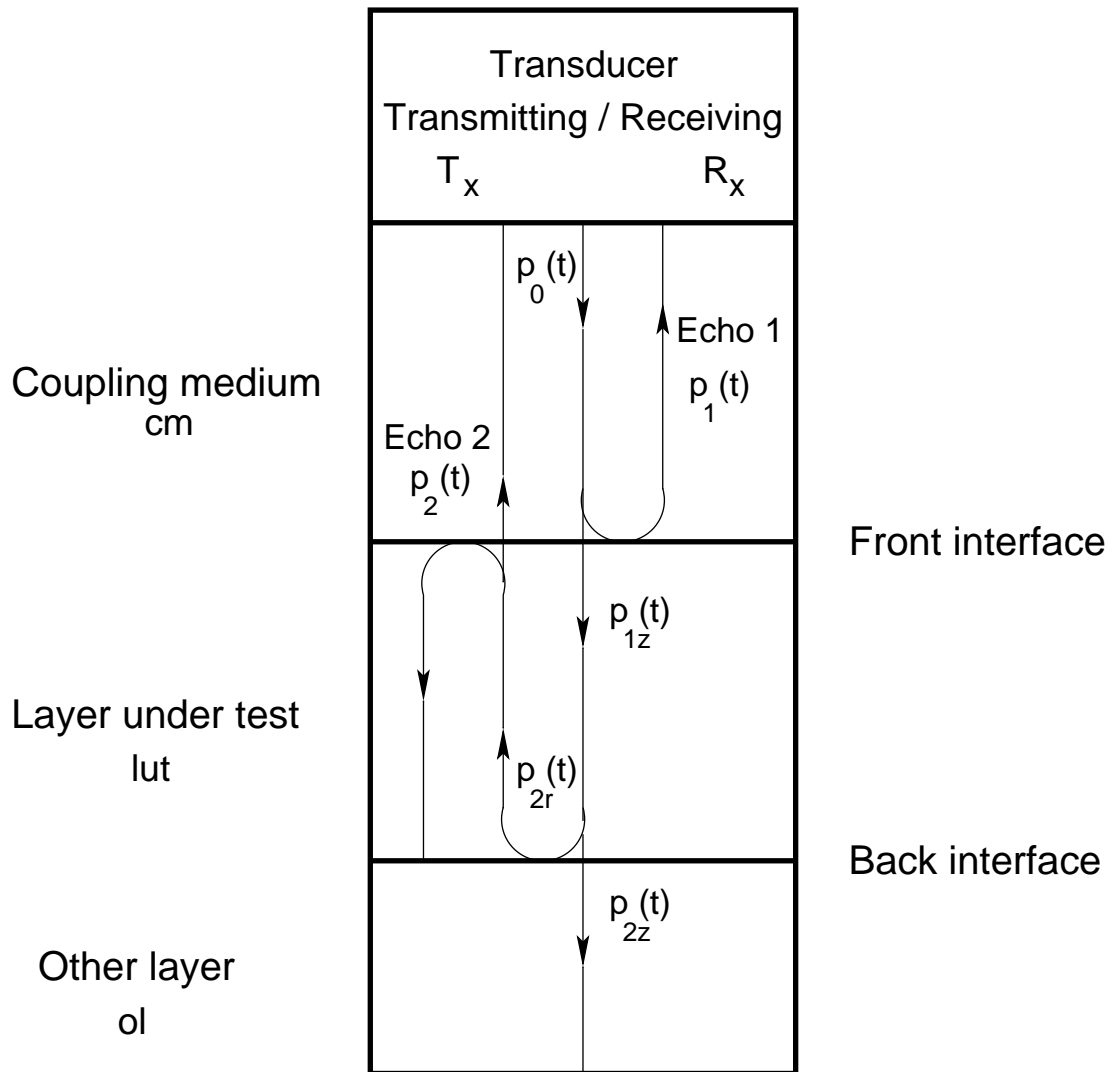


Figure 2.1: Echoes in a multilayer system

In the frequency range of operation, attenuation coefficient α can be assumed to be linearly related to frequency ($\alpha = aF$). In a multilayered system, with layers numbered as 1, 2, ..., N-1, N..., the transfer function for echoes from the front and back interfaces of layer 2 is given, using Eqn 2.11 and 2.12, as

$$H_{2,1}(F) = \frac{r_2(1 - r_1^2)}{r_1} H_{lut}^2(F) \quad (2.13)$$

$$= \frac{r_2(1 - r_1^2)}{r_1} e^{-2\alpha_2(F)L_2} e^{-j4\pi FL_2/c_2} \quad (2.14)$$

Similarly for layer N we have,

$$H_{N,N-1}(F) = \frac{r_N(1 - r_{N-1}^2)}{r_{N-1}} e^{-2\alpha_N(F)L_N} e^{-j4\pi FL_N/c_N} \quad (2.15)$$

where r_1, r_2, \dots, r_N are the reflection coefficients of layer interfaces 1, 2, ..., N respectively, L_N is the layer thickness, c_N is the velocity of propagation and α_N is the attenuation coefficient of layer L_N .

The layer transfer function is thus a complex quantity having a magnitude and phase information. The magnitude of the transfer function for the two echoes from a layer is related to reflection coefficients of the layer interfaces and the attenuation coefficient of the layer. The phase of the transfer function is related to the acoustic velocity in the layer. The most important point to be noted here is that if the echoes can be separated by time domain windowing, the echo transfer function obtained for a specific layer is independent of other layers and transducer characteristics.

2.4 Investigations reported earlier

This section reviews some of the reported work in the field of noninvasive temperature estimation using ultrasound.

Ultrasound velocity and attenuation were considered as promising parameters by Bowen [1]. Bowen's work estimated propagation velocity as a parameter for the use of thermometry. Davis and Lele [2] described an acoustic phase shift technique for the noninvasive measurement of temperature changes in tissues. The phase shift of an interrogating pulsed

ultrasonic sinusoidal wave is used to measure changes in the propagation velocity with respect to temperature.

Seip et al [7] discussed a noninvasive technique for monitoring tissue temperature changes due to heating fields, using diagnostic ultrasound. Though the effect of temperature on coupling medium was considered, transducer characteristics were not taken into account.

Satio et al [6] used B-mode ultrasound to analyze the attenuation of reflected ultrasound signal and concluded that with preliminary known characteristics of the temperature dependence of attenuation coefficient slope of the tissue of interest, it may be possible to measure the tissue temperatures noninvasively. They appear to have ignored the dependence of reflection coefficient on temperature.

Kak and Dines [5] described the estimation of single layer attenuation using pulsed ultrasound, using transmission technique. Different signal processing techniques for estimation of attenuation coefficient were discussed. Estimation of attenuation coefficient of a particular layer in a multilayered materials was not discussed.

Gadgil et al [3] [4] carried out investigations on ultrasound thermometry at IIT Bombay. The aim of the work was to identify parameters that could be used to monitor temperature of a layer of interest in a multilayered material, noninvasively. Estimation of acoustic velocity, attenuation coefficient, layer transfer function, layer impulse response, and RMS time duration were considered.

Presence of noise in the pulse echoes introduces a distortion in the transfer function and restricts the accuracy with which it can be determined. To minimize the effect of noise on the transfer function, the signal strength should be high. Broadband transducers, which are preferred in pulse echo systems due to their fast response times have low signal strength at high frequencies. This is due to the fact that attenuation is high at higher frequencies. To overcome this limitation and to improve the signal-to-noise ratio, several narrow band piezoelectric transducers covering different frequency bands were used by Gadgil [3].

Experiments were carried out on material layers of Perspex, PVC, and polypropylene. These layers were immersed in a water bath, the temperature of which could be controlled. The test materials were exposed to the set temperature for a sufficiently long time to ensure that thermal equilibrium was established. Water was constantly stirred to ensure uniform

temperature distribution. Pulsed ultrasound was incident on the test materials and the resulting echoes were acquired. This experiment was performed with multiple narrow band transducers with resonant frequencies at 1 MHz, 2 MHz, 3 MHz, and 5 MHz. Care was taken to minimize errors due to scattering, beam divergence, and inclination of transducers.

The acquired data were analyzed. The transfer function of the layer of interest was computed from the spectra of the echoes acquired from multiple transducers. The magnitude response for the transfer function was computed for each transducer in its frequency band. Portions of the response within the frequency band of the transducer were retained. The response was truncated at the crossover points of the neighboring transducer characteristics, as shown in Fig 2.2. Using extrapolation and curve fitting techniques a magnitude response over the desired frequency band was formed. It was observed that the magnitude response of the transfer function varies as a function of temperature as shown in Fig 2.3.

A number of parameters based on the transfer function and the impulse response were computed for temperature estimation. These parameters are, attenuation coefficient, RMS band width, RMS time duration, etc. Techniques for estimating the attenuation coefficient from these parameters were developed. These are described in the next section.

The work concluded that attenuation coefficient computed from the magnitude part of the transfer function is a potential parameter for monitoring temperature of a medium of interest, noninvasively.

2.5 Estimation of attenuation coefficient from transfer function

The following techniques were used by Gadgil et al for estimating the attenuation coefficient [3] [4] from echo transfer function for the layer under test :

1. Transfer function
2. RMS bandwidth
3. Transfer function energy ratio

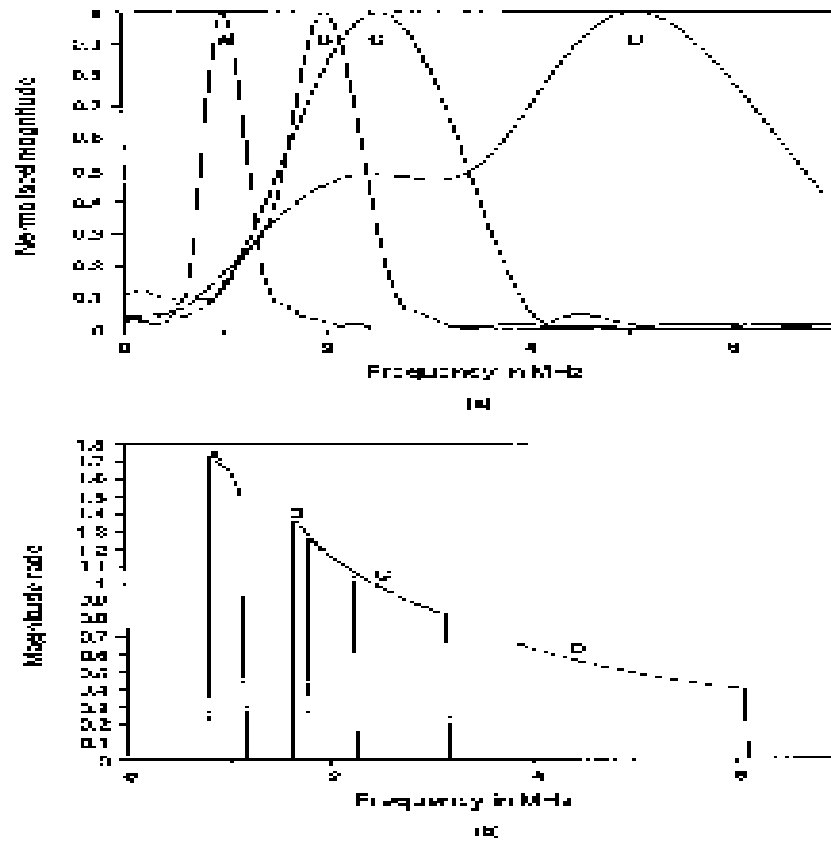


Figure 2.2: (a) Sensitivity characteristics of transducers A, B, C, D.
(b) Combined truncated magnitude division characteristics [3]

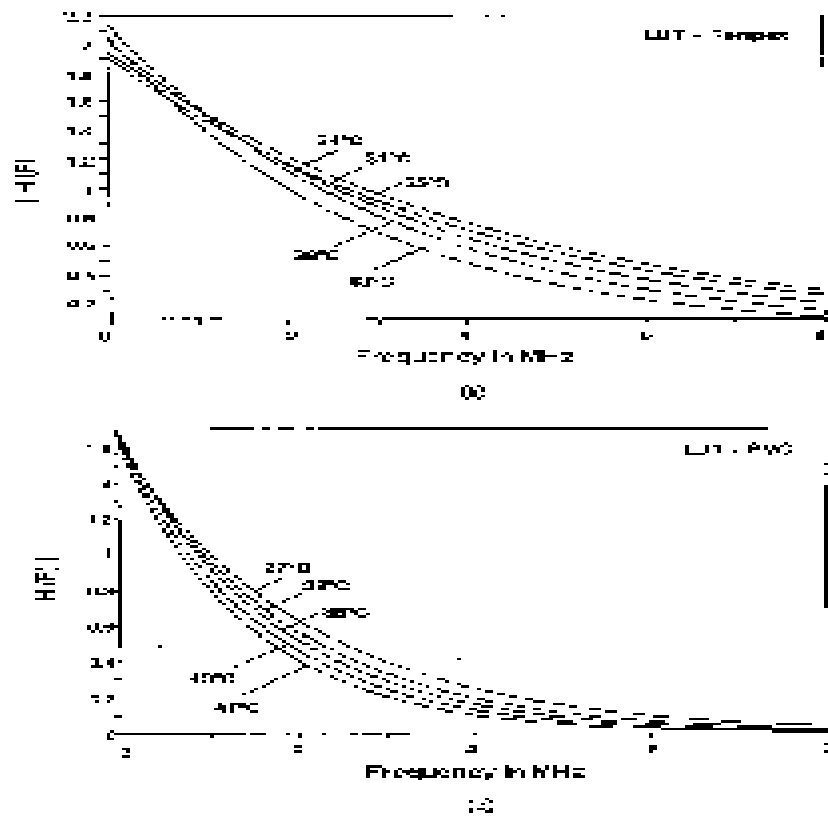


Figure 2.3: Effect of temperature on echo transfer function of Perspex and PVC [3]

4. Layer impulse response

5. RMS time duration

In all these methods, the attenuation coefficient of the layer under test, α_N , is modelled as a linear function of frequency.

$$\alpha_N = a_N F \quad (2.16)$$

a_N is the attenuation coefficient of the layer under test in dB/MHz-cm. It is further assumed that the reflection coefficient at both the interfaces are frequency independent.

Layer transfer function method

The attenuation coefficient can be computed from the magnitude part of the pulse echo transfer function as follows:

$$|H_{N,N-1}(F)| = \frac{V_N(F)}{V_{N-1}(F)} = \frac{r_N(1 - r_{N-1}^2)}{r_{N-1}} e^{-\alpha_N(F)2L_N} \quad (2.17)$$

Thus, attenuation coefficient is expressed as,

$$\alpha_N(F) = \frac{1}{2L_N} \left[\ln \frac{r_N(1 - r_{N-1}^2)}{r_{N-1}} - \ln \left(\frac{V_N(F)}{V_{N-1}(F)} \right) \right] \quad (2.18)$$

Attenuation coefficient computed by this technique requires apriori knowledge of reflection coefficients at the two interfaces.

RMS bandwidth method

RMS bandwidth, D_F is given by

$$D_F = \left[\frac{\int_0^\infty (F - F_m)^2 |H_{N,N-1}(F)|^2 dF}{\int_0^\infty |H_{N,N-1}(F)|^2 dF} \right]^{1/2} \quad (2.19)$$

where, F_m is a suitable reference frequency at which $|H(F)|^2$ is maximum. Here $F_m = 0$

Attenuation coefficient can be calculated from the RMS bandwidth and hence

$$a_N = \frac{\pi}{\sqrt{2} D_F L_N} \quad (2.20)$$

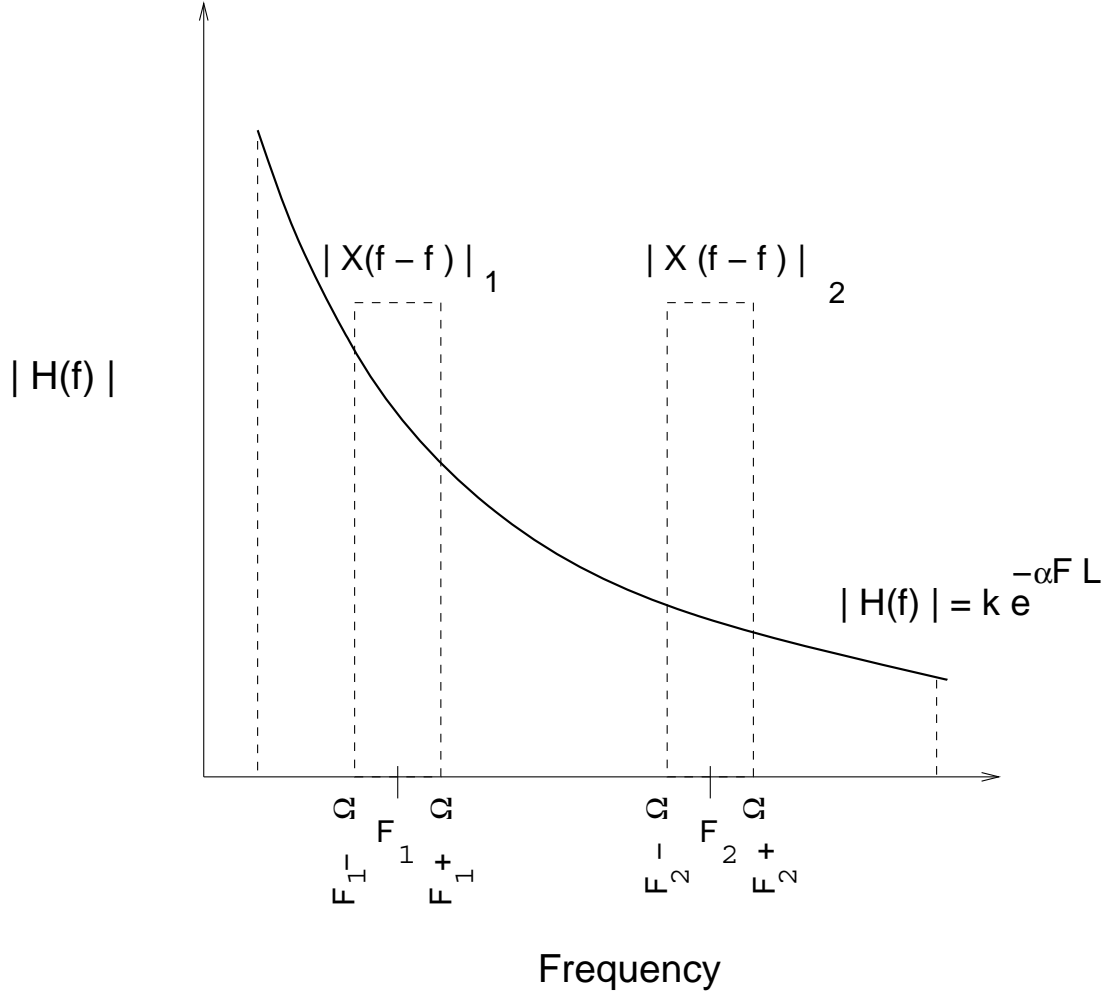


Figure 2.4: Use of weighting function for computation of attenuation coefficient

Transfer function energy ratio method

As shown in Fig 2.4. Two frequency bands each with a width of 2Ω centered around F_1 and F_2 respectively are selected. The magnitude part of the transfer function is given by Eqn 2.17.

Let $X(F)$ be a weighting function as shown in the Fig 2.4. Let E_1 and E_2 represent the weighted energy of $H_{N,N-1}(F)$ in the bands centered around F_1 and F_2 respectively.

$$E_1 = 2 \int_{F_1 - \Omega}^{F_1 + \Omega} |X(F - F_1)H(F)|^2 dF \quad (2.21)$$

$$E_2 = 2 \int_{F_2 - \Omega}^{F_2 + \Omega} |X(F - F_2)H(F)|^2 dF \quad (2.22)$$

The weighting function $X(F)$ can be used to emphasize those regions of frequency where the signal-to-noise ratio is much higher in transfer function $H(F)$. If $X(F)$ is selected to be constant over its bandwidth then energies E_1 and E_2 represent the energies in $H(F)$ for the two frequency bands respectively. Energy ratio E_1/E_2 is given by,

$$\frac{E_1}{E_2} = e^{4a_N L_N (F_2 - F_1)} \quad (2.23)$$

As seen from the above equation, the ratio of energies is a function of the attenuation coefficient of the material. Further, the ratio of energies is also a function of the dimensions of the material. Thus,

$$a_N L_N = \frac{1}{4(F_2 - F_1)} \ln\left(\frac{E_1}{E_2}\right) \quad (2.24)$$

The advantage of the transfer function energy ratio method is that it does not require knowledge of the reflection coefficients of the layer. Further, since energy of the received signals is computed by a process of integration over frequency bands with high SNR, this method would have a higher noise immunity as compared to the first two methods.

Impulse response

The layer impulse response is given by,

$$h_{N,N-1}(t) = \frac{r_N(1 - r_{N-1}^2)}{r_{N-1}\pi} \left[\frac{(a_N L_N / \pi)}{(a_N L_N / \pi)^2 + (t - [2L_N / c_N])^2} \right] \quad (2.25)$$

The maxima of the layer impulse response occurs at $t = t_c$. The maxima is given by,

$$h_{N,N-1}(t)_{max} = \frac{r_N(1 - r_{N-1}^2)}{r_{N-1}} \frac{1}{a_N L_N} \quad (2.26)$$

If t_1 and t_2 are instants of time in the impulse response curve where the values of the response are one half the peak values, the time difference $t_2 - t_1$ is given by,

$$t_2 - t_1 = \frac{2a_N L_N}{\pi} \quad (2.27)$$

a_N is given by the above equation as,

$$a_N = \frac{\pi(t_2 - t_1)}{2L_N} \quad (2.28)$$

RMS time duration

RMS time duration, D_t is given by [3] [4]

$$D_t = \left[\frac{\int_{-\infty}^{\infty} (t - t_m)^2 |h_{N,N-1}(t)|^2 dt}{\int_{-\infty}^{\infty} |h_{N,N-1}(t)|^2 dt} \right]^{1/2} \quad (2.29)$$

where, t_m is the time at which the peak of $h(t)$ occurs. Attenuation coefficient can then be obtained from the RMS time duration from the following Eqn [1]

$$a_N = \frac{\pi D_t}{L_N} \quad (2.30)$$

2.6 Estimation of temperature from attenuation coefficient

Gadgil et al [3] used the techniques discussed in the previous section to estimate temperature from the attenuation coefficient. The experimentally obtained value of the attenuation coefficient at different temperatures are given in Table 2.1 for Perspex, and PVC.

The relative change in the attenuation coefficient can be defined as,

$$S_a(\theta) = \frac{a(\theta) - a(\theta_0)}{a(\theta_0)} \quad (2.31)$$

where, $a(\theta)$ is the attenuation coefficient at temperature θ , $a(\theta_0)$ is the attenuation coefficient at reference temperature θ_0 .

The slope of the relative change can be given as,

$$\frac{S_a(\theta_2) - S_a(\theta_1)}{\theta_2 - \theta_1} = \frac{a(\theta_2) - a(\theta_1)}{a(\theta_1)} \frac{1}{\theta_2 - \theta_1} \quad (2.32)$$

where, $S_a(\theta_1)$ and $S_a(\theta_2)$ are the relative changes in the attenuation coefficient for temperatures θ_1 and θ_2 respectively. The corresponding attenuation coefficients are $a(\theta_1)$ and $a(\theta_2)$.

The slope of the relative attenuation coefficients over temperature range of 35 - 43°C for Perspex and PVC are given in Table 2.2, as calculated from the results obtained by Gadgil et al [3] [4].

Table-2.1 Attenuation coefficient for Perspex and PVC using different methods as a function of temperature

Temperature $^{\circ}\text{C}$	a , in dB / (MHz. cm)					
	Perspex			PVC		
	RMS Band width	RMS Time duration	Energy ratio	RMS Band width	RMS Time duration	Energy ratio
24	2	1.87	1.99	4.31	3.59	4.26
27	2.15	2.09	2.09	4.57	3.76	4.52
31	2.26	2.36	2.31	4.80	3.95	4.76
35	2.38	2.47	2.49	5.0	4.10	4.95
39	2.50	2.68	2.67	5.47	4.43	5.42
43	2.59	2.81	2.81	5.91	4.72	5.84
47	2.92	3.23	3.21	6.19	4.95	6.12

Table-2.2 Slope of relative change in attenuation coefficient, in percent/ $^{\circ}\text{C}$

Material	RMS Bandwidth	RMS time duration	Energy ratio
Perspex	1.147	0.735	1.071
PVC	1.516	1.260	1.498

Chapter 3

Investigations in ultrasound thermometry with a single transducer

3.1 Introduction

In techniques developed by Gadgil et al [3], temperature estimate of a material layer was obtained by obtaining the attenuation coefficient of the layer, by using a number of techniques, from the pulse echo transfer function of the layer. Further, in order to reduce the effect of noise, the method required the use of a large number of narrow band transducers, and the transfer function was computed from the response over the corresponding narrowbands by using extrapolation and curve fitting techniques. Due to the use of several transducers and involved signal processing, these techniques cannot be easily adapted for developing an instrumentation system for monitoring temperature noninvasively.

In this chapter a technique for estimating temperature of a material layer noninvasively, using a single transducer is proposed. In investigations by Gadgil [3], it was established that the magnitude part of the echo transfer function changes as a function of temperature as seen earlier in Fig 2.3. It is seen from this figure that this change is frequency dependent. For Perspex and PVC, the magnitude response appears to be relatively more sensitive to temperature in the 1 - 6 MHz frequency range. Thus on the basis of this observation, it may be possible to obtain a temperature estimate of a layer of interest from the transfer function itself, using a single transducer selected for high signal-to-noise ratio in the 1-6 MHz band.

The echo transfer function is computed in the region of confidence of the transducer and the magnitude and phase parts of the transfer function are investigated with an aim to identify parameters that could be used to estimate temperature noninvasively.

Temperature estimation from the magnitude and the phase part of the transfer function is discussed in Section 3.2 and 3.3 respectively. Experiments on the lines performed by Gadgil [3], were carried out with a 2.5 MHz narrowband transducer. The experimental setup and data acquisition procedure is described in Section 3.4. Data acquired from this experiment and those acquired by Gadgil [3], using a 5 MHz transducer are analyzed. The analysis performed on the acquired data is described in Section 3.5.

3.2 Estimation of temperature from phase part of the transfer function

Pulse velocity in a layer is a function of temperature, and it can be measured by measuring the propagation time. However, measure of pulse propagation time by measuring the time delay may have large errors due to the difficulty in defining the start of the received pulse. Here it is shown that we can get the same information from the phase part of the pulse echo transfer function. The pulse propagation time in the N^{th} layer is given by $t_N = L_N/c_N$ where c_N is the velocity in the layer and L_N is the acoustic path length. The phase shift at frequency F is therefore

$$\phi = ((2\pi F(2L_N/c_N))_{2\pi} \quad (3.1)$$

Therefore the phase is π at frequencies

$$F_\phi = (m + 0.25)\frac{c_N}{L_N}, m = 0, 1, 2, .. \quad (3.2)$$

If the thickness of the layer is known then the acoustic velocity can be estimated. Since c_N and L_N are functions of temperature, phase also is a function of temperature.

For a small temperature variation acoustic velocity as a function of temperature is given by [3]

$$c_{\theta_1} = c_{\theta_0}(1 - k_c\Delta\theta) \quad (3.3)$$

where, $\theta_1 = \theta_0 + \Delta\theta$ and k_c is the temperature coefficient of velocity. From Eqn 3.1, at π radians:

$$F_\phi(\theta_0) = (m + 0.25) \frac{c_{\theta_0}}{2L_{\theta_0}} \quad (3.4)$$

$$F_\phi(\theta_1) = (m + 0.25) \frac{c_{\theta_1}}{2L_{\theta_1}} \quad (3.5)$$

$$= (m + 0.25) \frac{c_{\theta_0}(1 - k_c\Delta\theta)}{2L_{\theta_0}(1 + k_L\Delta\theta)} \quad (3.6)$$

The frequency at which a phase of π occurs, reduces monotonically as the temperature of the layer increases. The relative change in $F_\phi(\theta_1)$ is given by

$$\begin{aligned} S_{F_\phi}(\theta) &= \frac{F_\phi(\theta_1) - F_\phi(\theta_0)}{F_\phi(\theta_0)} \\ &= \frac{-(k_c + k_L)\Delta\theta}{1 + k_L\Delta\theta} \\ &\approx -(k_c + k_L)\Delta\theta \end{aligned} \quad (3.7)$$

$S_{F_\phi}(\theta)$ is directly proportional to the change in temperature of the layer and is independent of the thickness of the layer.

It is to be noted that this method is a point measurement method, and may be prone to errors. Another way of measuring the frequency shift in the linear phase response is to obtain a cross correlation of the phase at temperature θ with that at reference temperature θ_0 , and note the position of the peak in the cross-correlation. This position will correspond to $F_\phi(\theta_1) - F_\phi(\theta_0)$.

3.3 Estimation of temperature from magnitude part of the echo transfer function

As seen in Section 2.3, the magnitude part of the echo transfer function is a function of the reflection coefficient of the layer and its attenuation coefficient. These parameters are a function of temperature. Thus the magnitude of the echo transfer function is also a function of temperature.

As observed from the analysis performed by Gadgil [3], the magnitude part appears to be relatively more sensitive in the 1 - 6 MHz frequency range. Thus, the mean squared

echo transfer function is computed in this frequency range. This is plotted as a function of temperature of the layer. The mean squared pulse echo transfer function in a frequency band defined by frequencies F_1 and F_2 is given by the following equation,

$$|H_{avg}^2(\theta)| = \frac{1}{F_2 - F_1} \int_{F_1}^{F_2} |H_{\theta}^2(F)| dF \quad (3.8)$$

3.4 Experimental setup

The experimental setup is shown in Fig 3.1. It consists of a transceiver and a 2.5 MHz ultrasonic transducer immersible in water, for sending pulsed ultrasound on to the test material in water and receiving echoes. The test material used is Perspex. It is an amorphous material with acoustic properties comparable to biological tissues. Care is taken to ensure that throughout the experiment, the axis of the piezoelectric transducer is coincident to that of the Perspex block. The temperature of the water bath is raised from room temperature to various test temperatures, the maximum temperature being 50 °C (a temperature range of 28 to 50 °C was covered). The water is constantly stirred to ensure uniform heating. The resulting echoes at these temperatures are amplified and acquired using a digital storage scope. This procedure is repeated for different thicknesses of the Perspex block.

A transmitter (Panametrics transceiver model 5052UA) is used to excite the piston type transducer with sufficient energy to receive the echoes from the top and bottom surfaces of the test material. The pulse repetition rate is so adjusted that reflections due to subsequent excitation pulses do not interfere with the previous reflections. The pulse duration is set at 720 nsec.

The acoustic pressure wave, produced by the transducer travels through the coupling medium to the test material. There is an acoustic mismatch at the interface formed by the coupling medium and the top surface of the test medium. Due to this mismatch some of the incident energy is reflected and is then picked up by the same transducer. In the receiving mode, transducer converts this reflected pressure wave into an electrical signal. Similarly, from the other interface of the test medium one more reflection occurs. At the first interface some part of this reflected signal gets reflected back into the test material while remaining ultrasonic energy enters into the coupling medium layer and is then picked up and converted

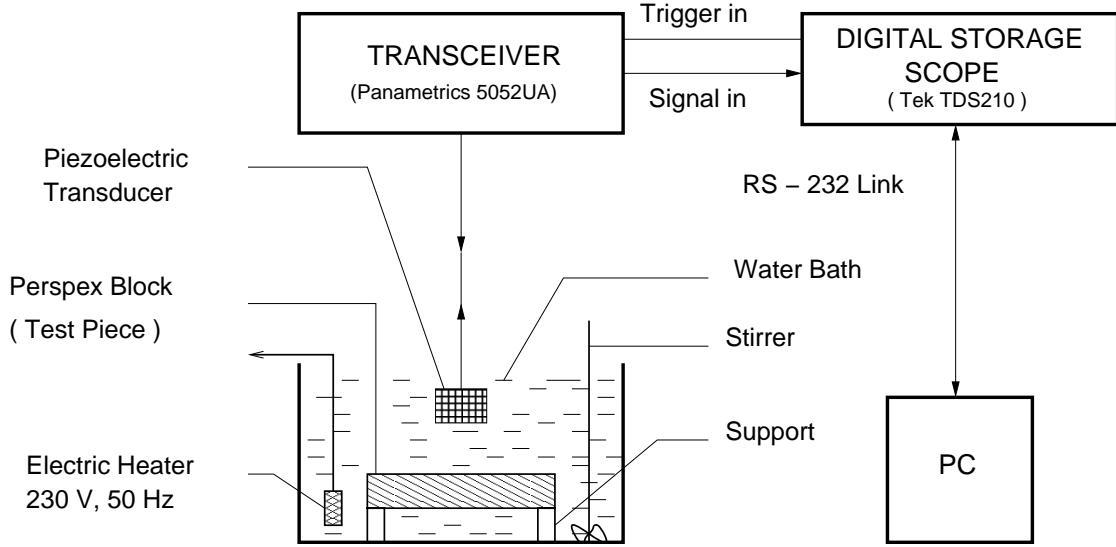


Figure 3.1: Experimental setup

by the same transducer. The signals picked up by the transducer in the receiving mode are amplified by a wide band amplifier and acquired by a digital storage scope (Tektronix model). The digital storage scope samples the signal at a rate of 100 MSa/s. Signals are acquired starting with a delay with respect to the trigger pulse received from the transceiver. The trigger pulse is a TTL pulse generated in synchronism with the transmitted pulse. The delay is adjusted such that echoes from the two interfaces remain within the acquired signal segment over the temperature range of interest. This delay remains constant for all the recordings for a particular sample so that the velocity measurements based on relative time shift or phase shift can be made. Signal samples of width 2.5 K are acquired. The acquired signal segments are ensemble averaged over 128 recordings and transferred to a PC via a RS-232 link for further processing.

3.5 Signal processing

The signals acquired using the experimental setup described in the preceding section, as well as those acquired by Gadgil [3] using a 5 MHz transducer were analyzed using signal processing package Matlab.

The first step was separation of the two echoes. The sample values other than those in the two echoes of interest are set to zero. This signal waveform is used to obtain two signals. In the first signal, only the echo from the first interface is retained, all the other sample values are set to zero. In the second signal, only the echoes from the second interface is retained. The magnitudes of all other sampled points are set to zero, to reduce the noise related errors in processing. The width and position of the gating pulses for obtaining the two signals should remain constant for all the signals for a given sample. An example of these split signals is shown in Fig 3.2.

In the next step, the Fourier transforms of the split signals(acquired at different temperatures of the test medium) in the form of magnitude and phase were computed.

Finally, the spectra of the two echoes is analyzed as described below:

1. The transfer function($H(F)_{2,1}$) as derived in Eqn 2.15, which is the ratio of the Fourier transform of the echo from the second interface to the Fourier transform of the echo from the first interface is computed. Care is taken to ensure that divide-by-zero errors are avoided.
2. The frequency at which a phase shift of π radians occurs (F_ϕ), is plotted as a function of temperature.
3. Cross-correlation of the phase response with the phase response at temperature θ_0 is carried out, and the point at which the peak in the cross correlation function occurs ($F_{\phi CC}$) is noted as a function of temperature.
4. It was found that for a 5 MHz transducer the change in the pulse echo transfer function as a function of temperature is maximum in the frequency band defined by the frequencies : 1.42 MHz and 6 MHz. For a 2.5 MHz transducer the corresponding frequencies are : 2.5 MHz and 2.8 MHz. The mean squared transfer function, as described in Section 3.3, is computed and plotted as a function of temperature. For a 2.5 MHz transducer, the transfer function is defined for a bandwidth of 2.5-2.8 MHz. For a 5 MHz transducer the mean squared transfer function is defined for a bandwidth of 1.42-6 MHz

5. As discussed in Section 2.5, energy ratio E_{R1} of the transfer function is computed from the magnitude spectra of the echoes. For signals acquired using 2.5 MHz transducer in the author's setup, the frequency bands used are: 0.89-1.25 MHz and 2.32-2.67 MHz. For signals acquired using 5 MHz transducer in the setup by Gadgil [3], the frequency bands are : 2.8-3.57 MHz and 5-5.7 MHz.

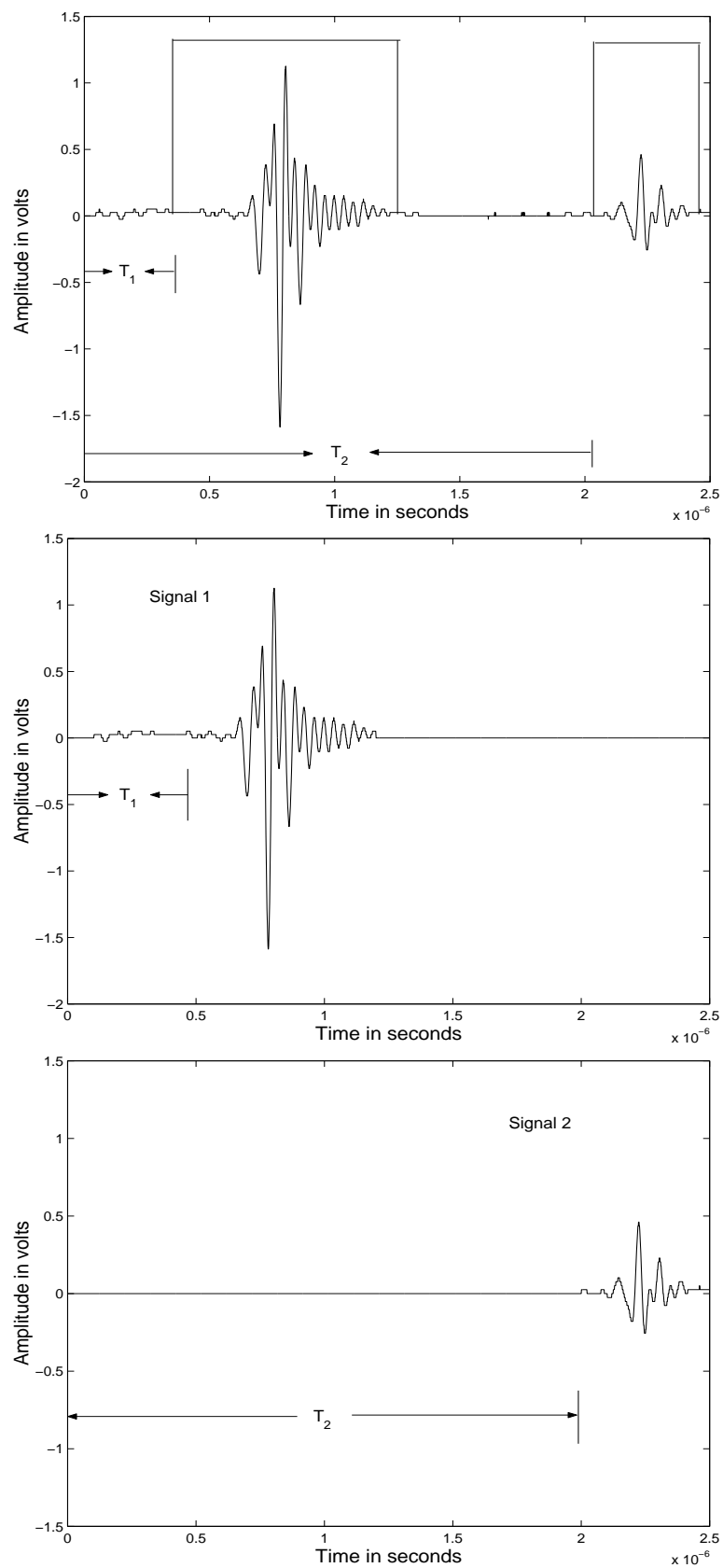


Figure 3.2: The signal received by the transducer and the two gated echoes

Chapter 4

Results and discussions

4.1 Results

This chapter presents the results of the analysis of the data obtained. These data correspond to single layered and multilayered samples of Perspex and PVC.

For estimating temperature θ noninvasively, the following techniques were investigated,

1. Transfer function energy ratio (as described in Section 2.5)
2. Phase Response method (as described in Section 3.2)
3. Mean squared transfer function (as described in Section 3.3)

4.2 Transfer function energy ratio method

The transfer function energy ratio method was discussed in Sections 2.5. Referring to Fig 2.4, for experiments performed with 2.5 MHz transducer, $F_{1-\Omega}= 0.89$ MHz, $F_{1+\Omega}= 1.25$ MHz, $F_{2-\Omega}= 2.32$ MHz, $F_{2+\Omega}= 2.67$ MHz For experiments performed with a 5 MHz transducer $F_{1-\Omega}= 2.8$ MHz, $F_{1+\Omega}= 3.57$ MHz, $F_{2-\Omega}= 5$ MHz, $F_{2+\Omega}= 5.7$ MHz Plots of energy ratio (E_{R1}) versus temperature (θ) for Perspex of thicknesses 5 mm, 10 mm, 15 mm, 20 mm, 25 mm are given in Fig 4.3-4.5. The graphs indicate monotonic trend but do not show repeatability. This is due to the fact that the energy ratio was computed over a narrow

frequency band of a single transducer. The energy ratio for samples mentioned in Tables 4.1 and 4.2 was also computed. The graphs in these cases also showed a nonrepeatable behavior.

4.3 Phase response method

As described in Chapter 3, the phase response of a medium interrogated by pulsed ultrasound is a function of temperature. This is seen from Fig 4.1, where the phase response at different temperatures (32°C, 35°C, 40°C, 43°C, 45°C) is plotted for a water/Perspex/water sample (layer of interest - Perspex of 20 mm thickness). From this figure, it is observed that the frequency (F_ϕ) at which a phase shift of π radians occurs changes as a function of temperature. While the shift in the phase response with temperature is the same for all phase shifts in the interval of $-\pi$ to $+\pi$, frequency at which a phase shift of π radians occurs is taken as a reference as it is convenient. The frequency at which a phase shift of π radians occurs is plotted as a function of temperature for water/Perspex/water sample, thickness of which being 15 mm, 20 mm, 25 mm in Fig 4.6. From this figure it is seen that there is a monotonic decrease in F_ϕ with temperature. However it is a function of the thickness of the sample. From equation 2.27 the ratio $S_{F_\phi}(\theta)$ is independent of the acoustic path length of the layer of interest (in this case Perspex). This ratio is plotted as function of temperature. This is shown in Fig 4.7. From this figure it is observed that for different thicknesses, the quantity $S_{F_\phi}(\theta)$ is independent of the acoustic path length of the material, and it monotonically decreases with temperature.

The data acquired by Gadgil [3] were also analyzed using this method. Fig 4.8 and 4.9 show the relation between F_ϕ versus temperature and $S_{F_\phi}(\theta)$ versus temperature for a thickness of 5 mm and 10 mm thickness of Perspex. These graphs also show that both F_ϕ and $S_{F_\phi}(\theta)$ decrease monotonically with temperature.

Single layered sample of PVC and multilayered samples of Perspex and PVC were analyzed in the same way as the above mentioned samples. The results of the analysis for Perspex and PVC layers of thicknesses 10 mm are shown in Fig 4.10 to 4.19. From these figures, it is seen that F_ϕ and S_{F_ϕ} reduce monotonically with temperature. Further the relative variation in F_ϕ is independent of the acoustic path length for all the samples.

From the tables it is seen that the temperature sensitivity of $S_{F\phi}(\theta)$ lies in the range of 0.11-0.18 percent/ $^{\circ}\text{C}$ for Perspex. For PVC it is between 0.17-0.18 percent/ $^{\circ}\text{C}$.

4.4 Mean squared transfer function

As described in Section 3.3, the mean squared pulse echo transfer function $|H_{avg}^2(\theta)|$ is plotted as a function of temperature θ for single layered and multilayered PVC samples. Relative variation in the mean squared pulse echo transfer function $S_{H^2avg}(\theta)$ is also plotted as a function of temperature. These graphs are shown from Fig 4.20 to Fig 4.33. For a 5 MHz transducer, the function showed a monotonic decrease in the 1.42 - 6 MHz frequency band. For a 2.5 MHz transducer the function showed a monotonic decrease in the 2.5-2.8 MHz frequency band. This monotonic decrease is observed for all samples. Further, $|H_{avg}^2(\theta)|$ is also a function of the thickness of the medium of interest and at lower thicknesses has a larger value. The slope of the relative variation in the mean squared transfer function for Perspex and PVC samples is given in Tables 4.1 and 4.2 respectively.

4.5 Discussions

The following techniques were investigated for estimating the temperature of a layer in single layered and multilayered sample from the pulse echo transfer function obtained using a single transducer.

1. Transfer function energy ratio method
2. Phase response method
3. Mean squared pulse echo transfer function

Transfer function energy ratio method

Transfer function energy ratio method did not show monotonicity for the samples used. This is due to the fact that this ratio was computed using a single transducer. A larger frequency band would have to be used for using this technique for estimating temperature. This would require the use of more than one transducer.

Table 4.1- Slope of relative changes in F_ϕ and H_{avg}^2 , in percent/ 0C , for different layers/thicknesses/transducers/experimental setup (Layer of interest - Perspex)

Sr.No.	Sample	Thickness (mm)	Ref. Fig. nos.	$\frac{\Delta S_{F_\phi}(\theta)}{\Delta \theta}$	Ref. Fig. nos.	$\frac{\Delta S_{H_{avg}^2}(\theta)}{\Delta \theta}$
1	W ¹ -P _X ² -W*	15	4.7	-0.143	4.21	-2.17
2	W-P _X -W*	20	4.7	-0.152	4.21	-1.57
3	W-P _X -W*	25	4.7	-0.116	4.21	-2.62
4	W-P _X -W**	5	4.9	-0.154	4.23	-1.13
5	W-P _X -W**	10	4.9	-0.133	4.23	-1.85
6	W-P-W-P _X -A ^{4**}	10	4.11	-0.176	4.25	-1.98
7	W-P _X -W-P-A**	10	4.13	-0.106	4.27	-2.07

1 - WATER 2 - PERSPEX 3 - PVC 4 - AIR

* - DATA ACQUIRED USING 2.5 MHZ TRANSDUCER, ** - DATA ACQUIRED USING 5 MHZ TRANSDUCER

Table-4.2 Slope of relative changes in F_ϕ and H_{avg}^2 , in percent/ 0C , for different layers/thicknesses/transducers/experimental setup (Layer of interest - PVC)

Sr. No.	Sample	Thickness (mm)	Ref. Fig.nos.	$\frac{\Delta S_{F_\phi}(\theta)}{\Delta \theta}$	Ref. Fig.nos.	$\frac{\Delta H_{avg}^2(\theta)}{\Delta \theta}$
1	W-P-W**	5	4.15	-0.181	4.29	-3.40
2	W-P-W**	10	4.15	-0.172	4.29	-2.87
3	W-P-W-P-A**	10	4.17	-0.182	4.31	-1.78
4	W-P _X -W-P-A**	10	4.19	-0.184	4.33	-2.76

1 - WATER 2 - PERSPEX 3 - PVC 4 - AIR

* - DATA ACQUIRED USING 2.5 MHZ TRANSDUCER, ** - DATA ACQUIRED USING 5 MHZ TRANSDUCER

Phase response method

In the phase response method, the frequency F_ϕ at which phase shift of π occurs is plotted against temperature in the 28-50 0C range. A monotonic relationship between $F_\phi(\theta)$ and

temperature θ is observed. We see that the relative sensitivity of this method is independent of layer thickness, in conformity with the theoretical analysis. The sensitivity obtained is between 0.106 and 0.176 percent/ $^{\circ}\text{C}$ for Perspex and between 0.172 and 0.184 percent/ $^{\circ}\text{C}$ for PVC. From the data reported earlier by Gadgil [3], the sensitivity for velocity is 0.13 percent/ $^{\circ}\text{C}$ for Perspex and 0.15 $^{\circ}\text{C}$ percent/ $^{\circ}\text{C}$ for PVC. Therefore one may conclude that the phase response method gives a measure closely related to variation in velocity.

Mean squared pulse echo transfer function

The mean squared pulse echo transfer function ($|H_{avg}^2(\theta)|$) was also computed. It was found that for a 5 MHz transducer, $|H_{avg}^2(\theta)|$ for both Perspex and PVC decreases monotonically with temperature in the 1.42- 6 MHz frequency band. This behavior was observed in case of multilayered samples also. For a 2.5 MHz transducer too, the above function showed a monotonically decreasing trend with temperature. The best frequency range for calculating $|H^2_{avg}|$ using the 2.5 MHz transducer was found to be 2.5-2.8 MHz. The mean squared transfer function is a function of the thickness of the medium of interest. The temperature sensitivity of $H_{avg}^2(\theta)$ for Perspex was found to be 1.13-2.62 percent/ $^{\circ}\text{C}$. For PVC the temperature sensitivity was found to be 1.78-3.4 percent/ $^{\circ}\text{C}$. The temperature sensitivity of attenuation coefficient [from Table 2.2] for Perspex was found to be 1.07 percent/ $^{\circ}\text{C}$. For PVC it was found to be 1.49 percent/ $^{\circ}\text{C}$.

Thus it is seen that the temperature sensitivity of relative change in $H^2_{avg}(\theta)$ is similar to the temperature sensitivity for attenuation obtained using multiple transducer method.

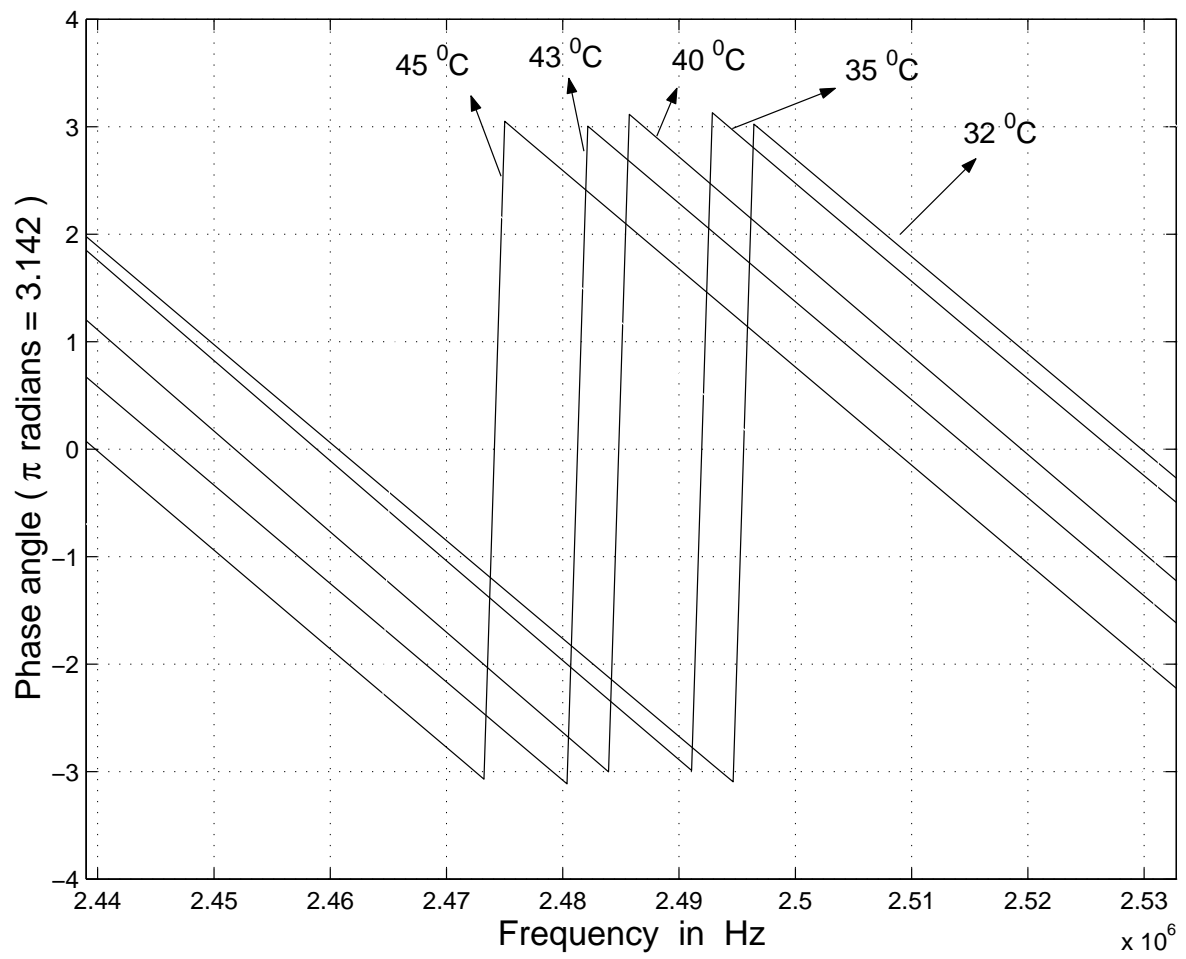


Figure 4.1: Dependence of phase response of transfer function vs temperature. Perspex layer of 20 mm thickness. Transducer 2.5 MHz

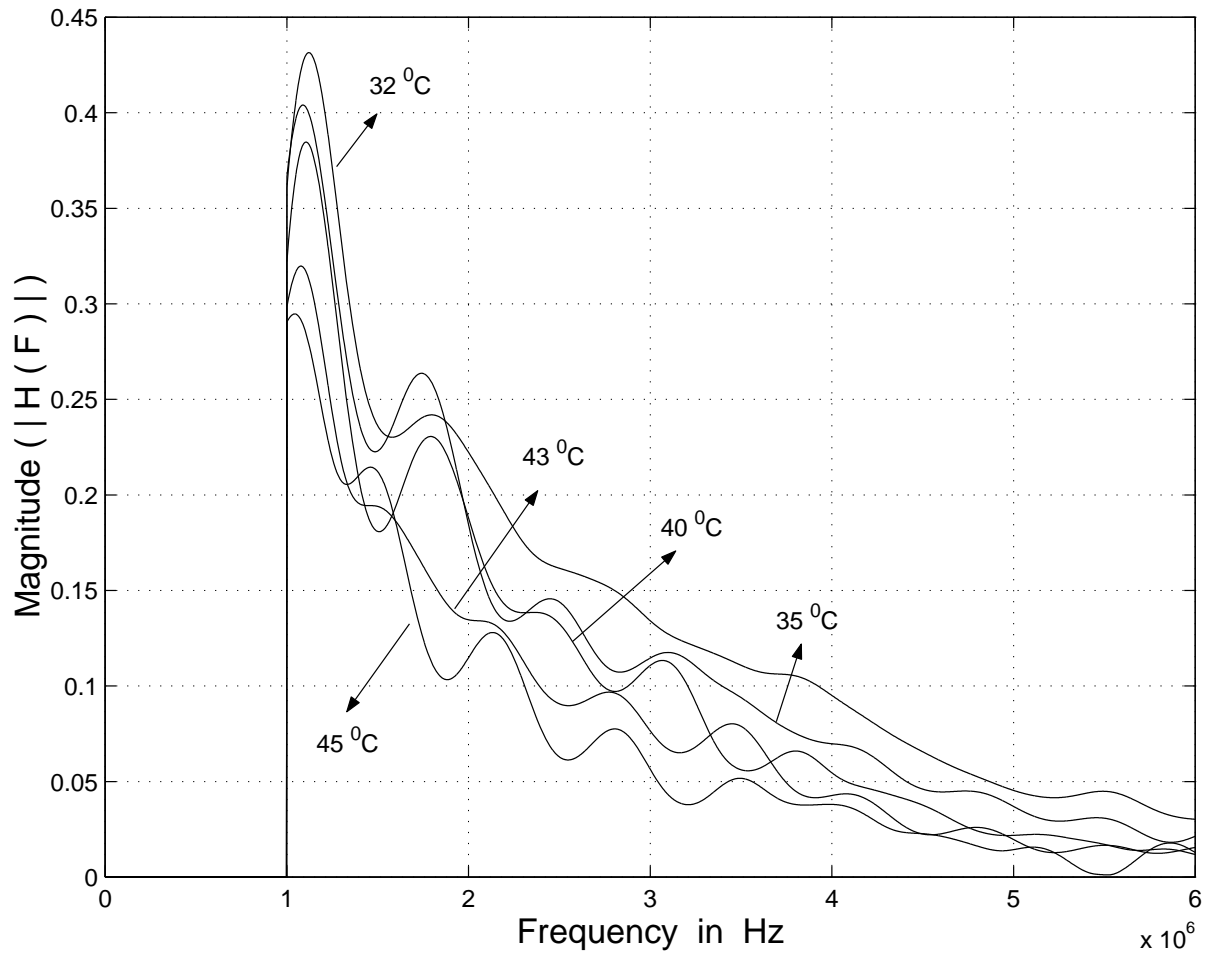


Figure 4.2: Dependence of magnitude response vs temperature. Perspex layer of 20 mm thickness . Transducer 2.5 MHz

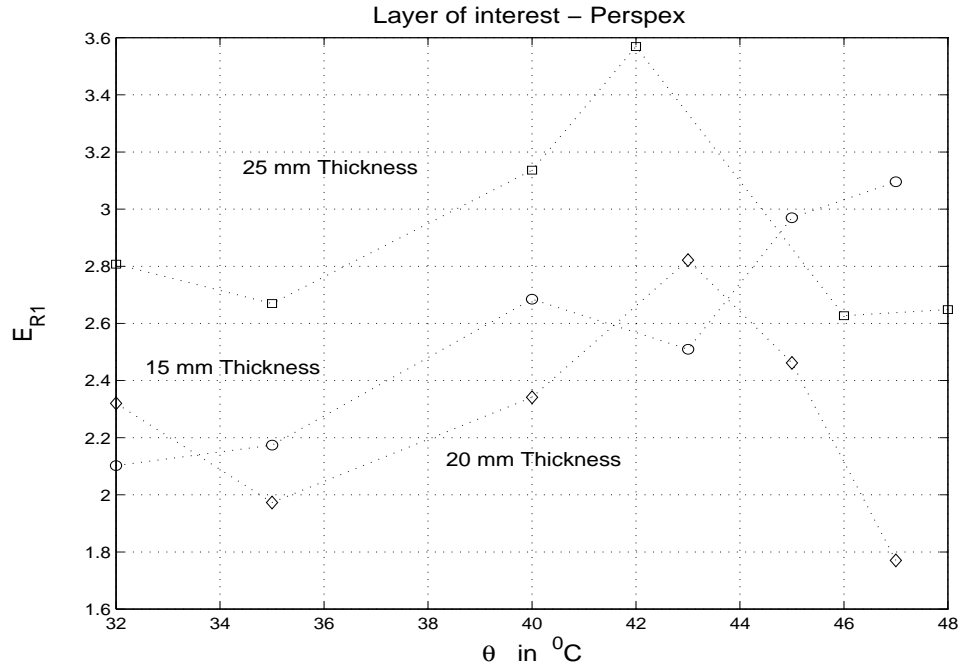


Figure 4.3: E_{R1} versus temperature θ for Water/Perspex/Water sample

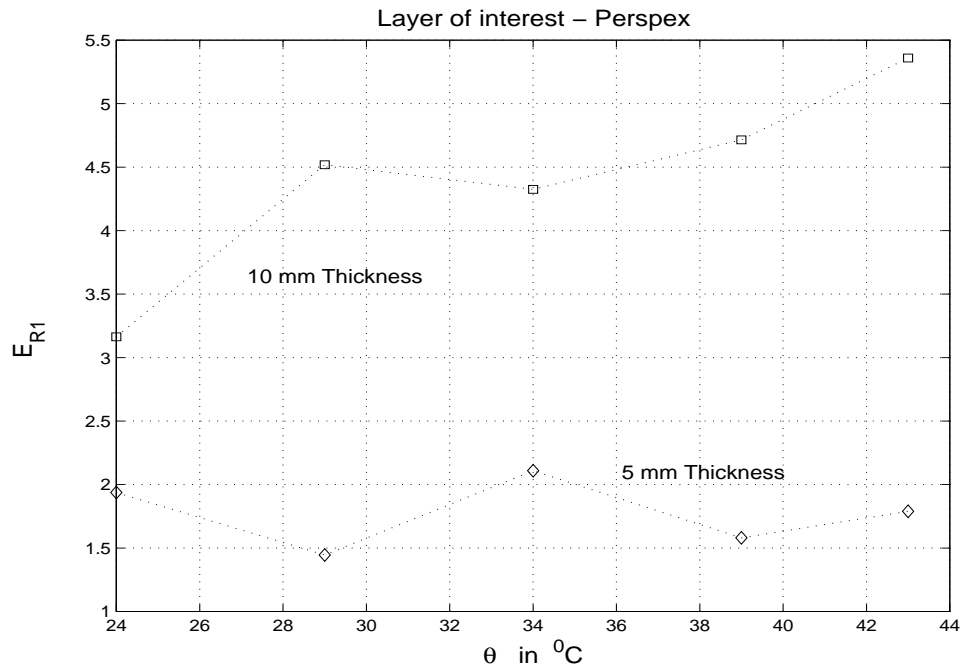


Figure 4.4: E_{R1} versus temperature θ for Water/Perspex/Water sample

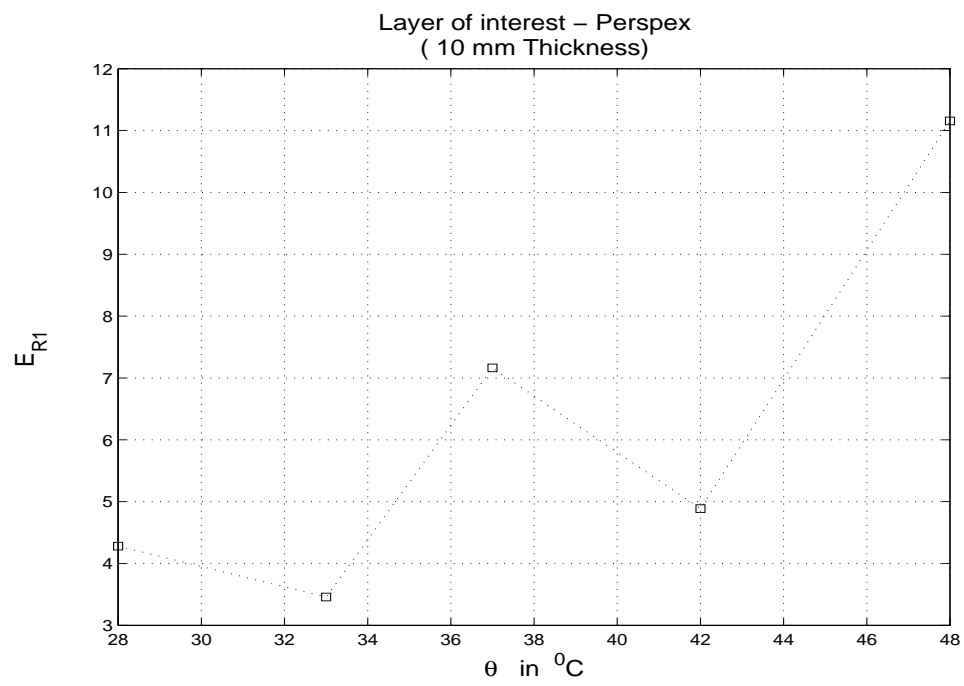


Figure 4.5: E_{R1} versus temperature θ for Water/PVC/Water/Perspex/air sample

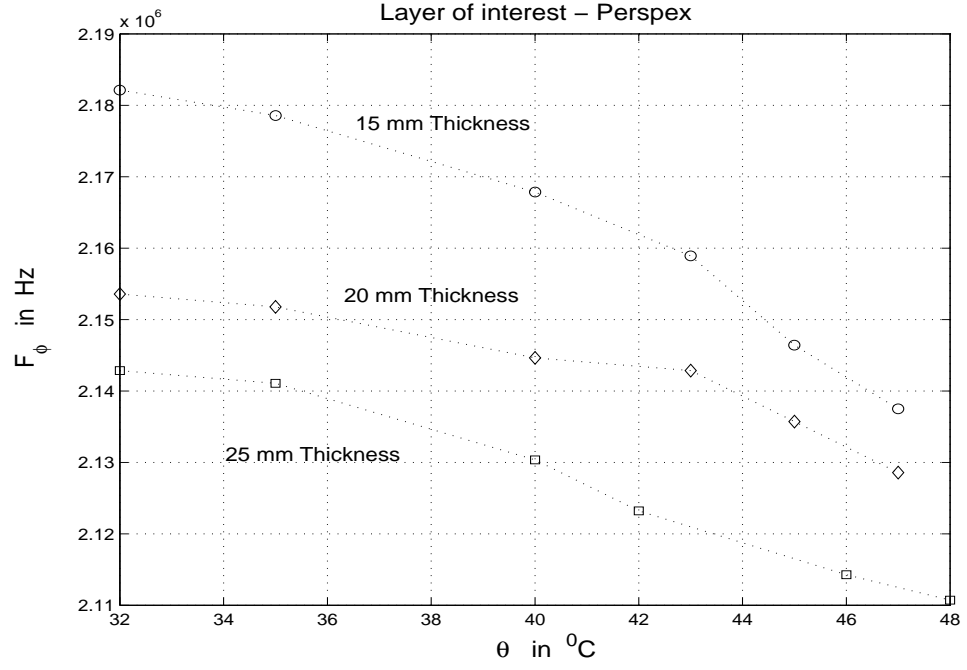


Figure 4.6: F_ϕ versus temperature θ for a water/Perspex/water sample [Table 4.1, sample 1-3]

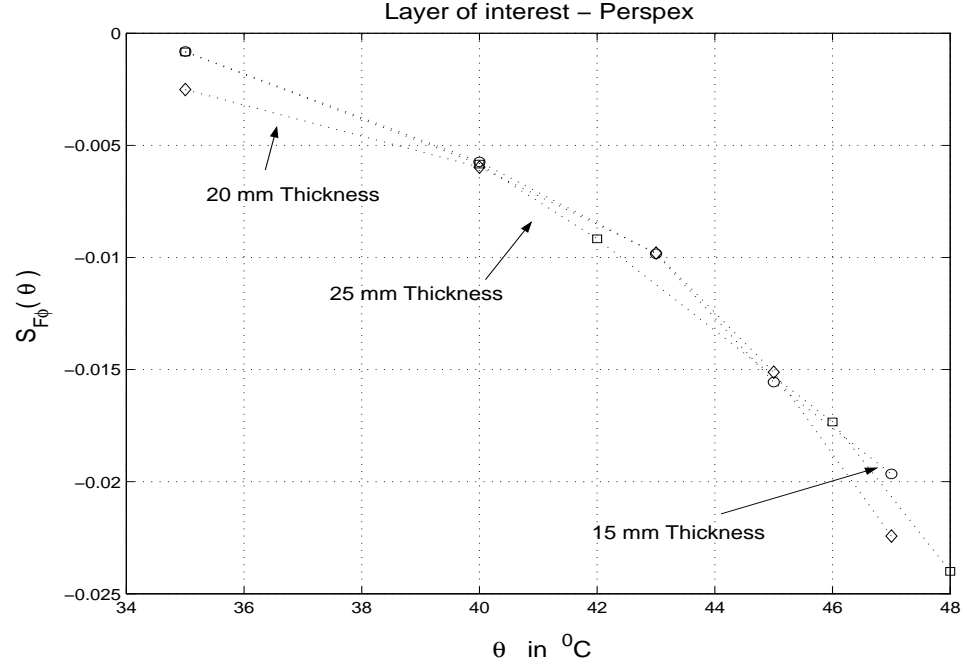


Figure 4.7: $S_{F_\phi}(\theta)$ versus temperature θ for a water/Perspex/water sample [Table 4.1, sample 1-3]

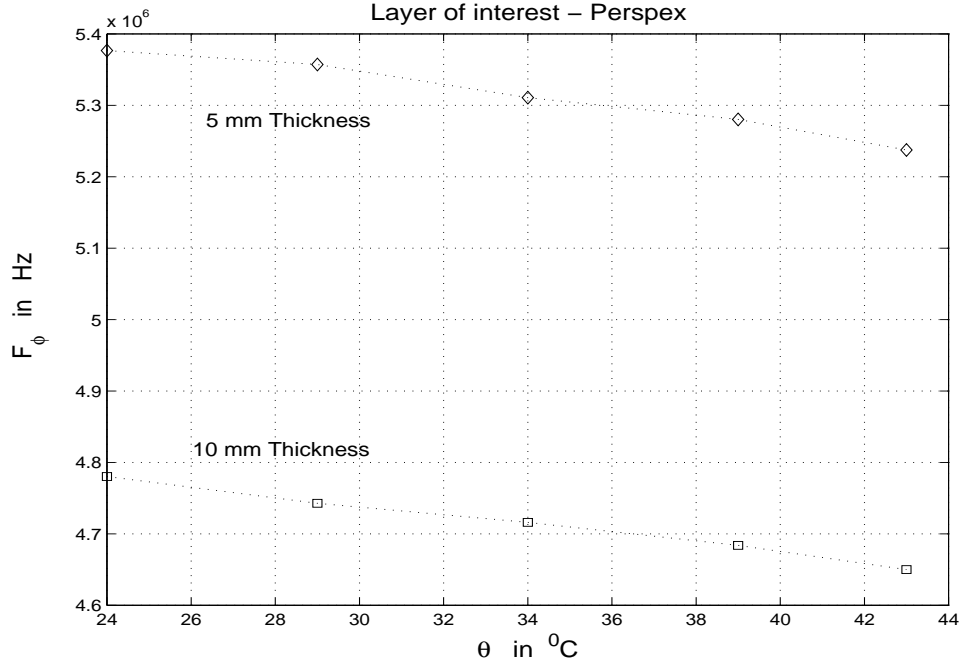


Figure 4.8: F_ϕ versus temperature θ for a water/Perspex/water sample [Table 4.1, sample 4-5]

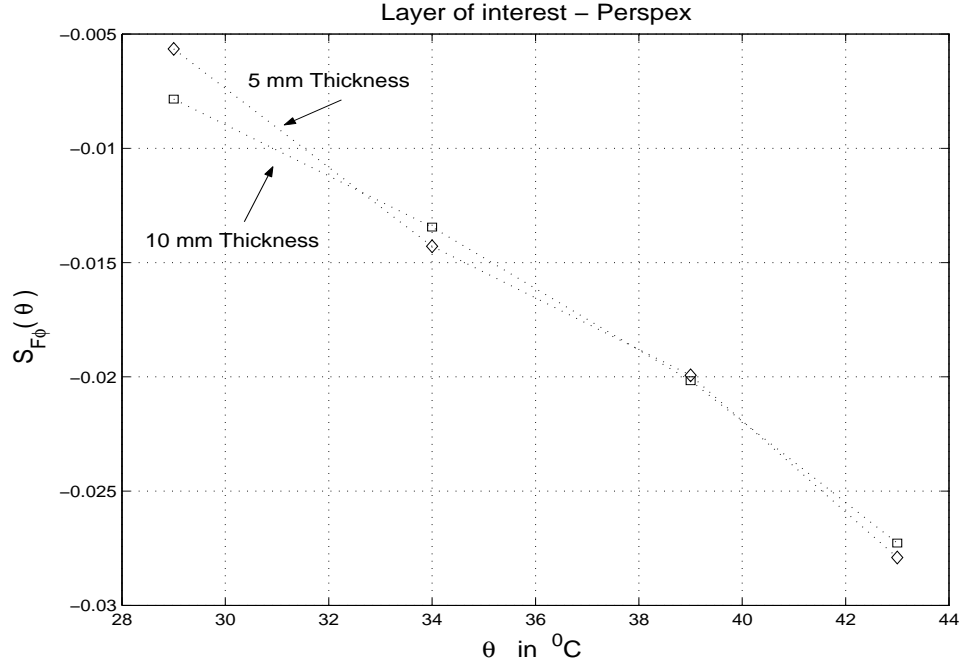


Figure 4.9: $S_{F_\phi}(\theta)$ versus temperature θ for a water/Perspex/water sample [Table 4.2, sample 4-5]

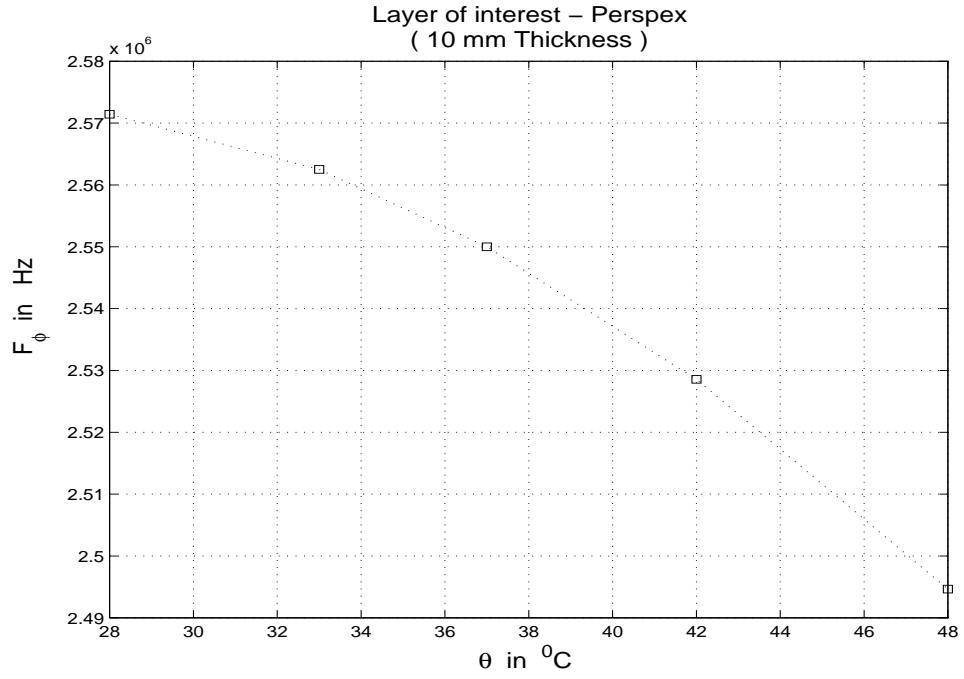


Figure 4.10: F_{ϕ} versus temperature θ for a multilayered water/PVC/water/Perspex/air sample [Table 4.1, sample 6]

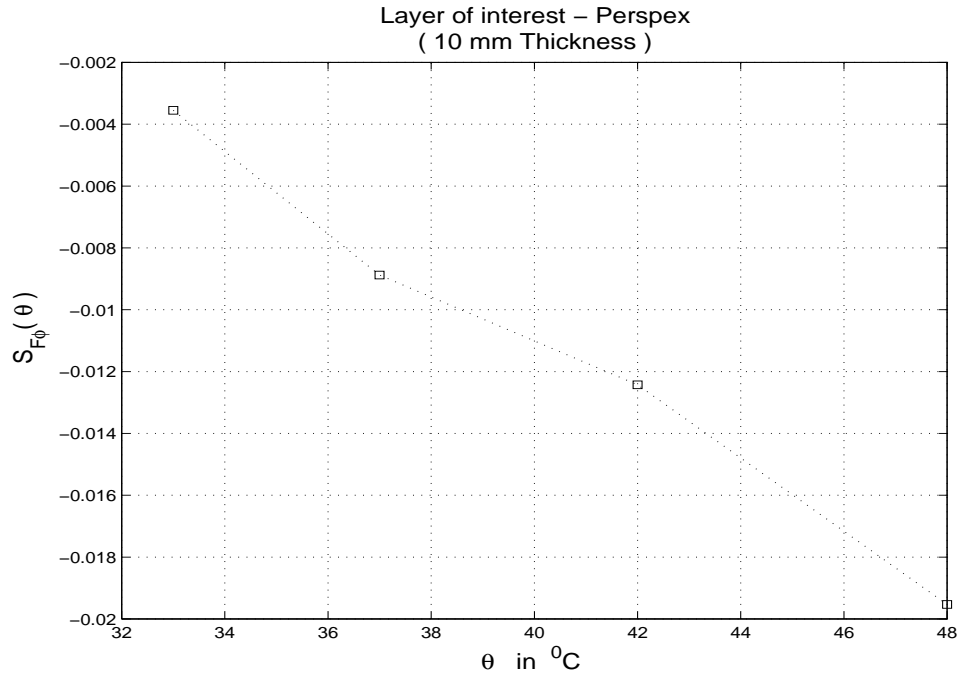


Figure 4.11: $S_{F_{\phi}}(\theta)$ versus temperature θ for a multilayered water/PVC/water/Perspex/air sample [Table 4.1, sample 6]

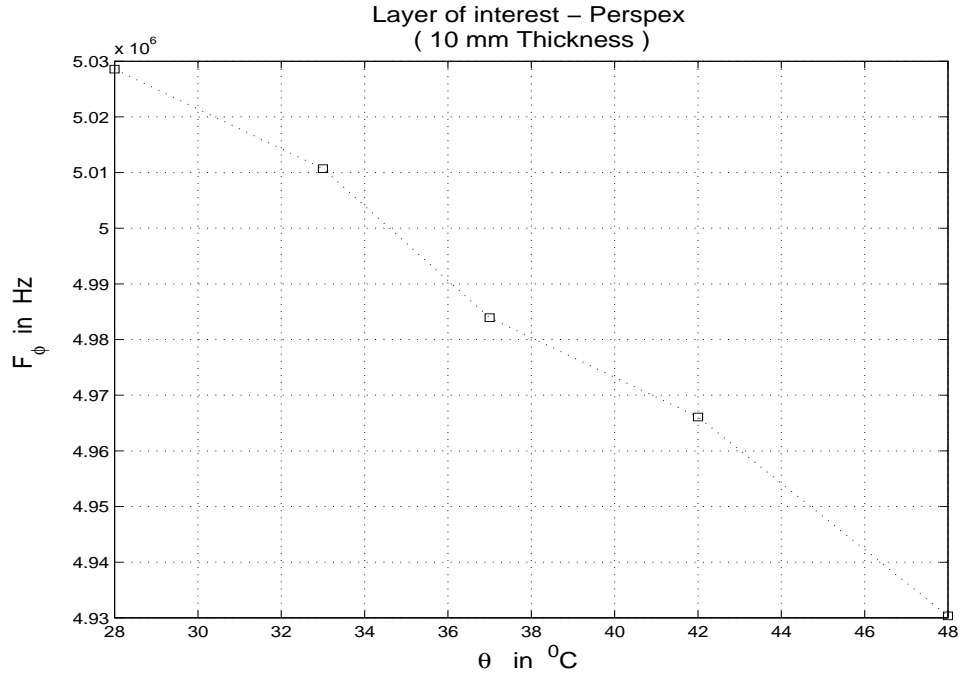


Figure 4.12: F_{ϕ} versus temperature θ for a multilayered water/Perspex/water/PVC/air sample [Table 4.1, sample 7]

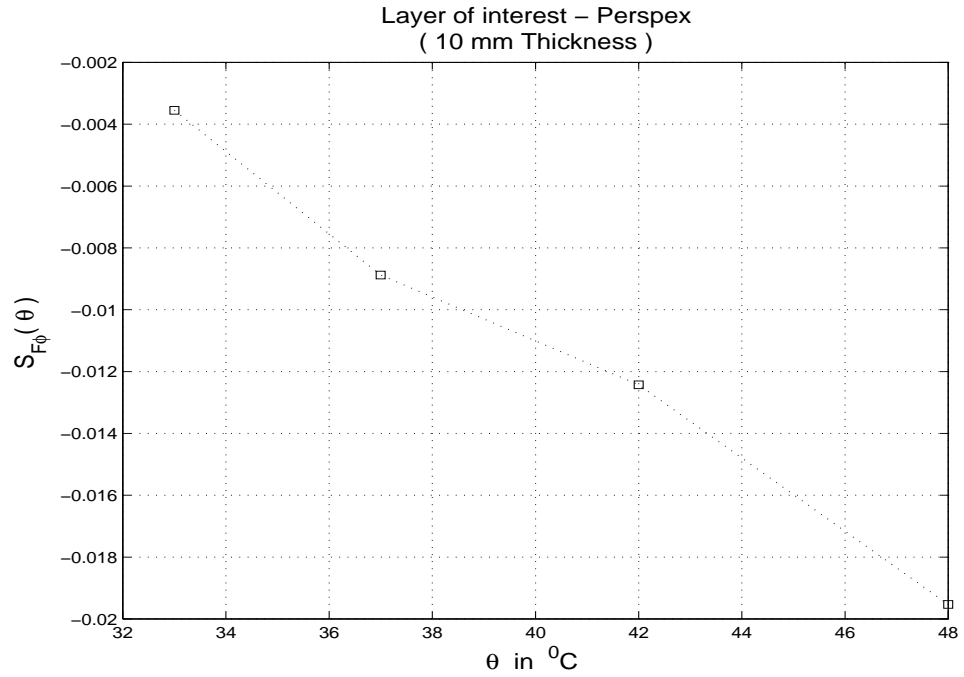


Figure 4.13: $S_{F_{\phi}}(\theta)$ versus temperature θ for a multilayered water/Perspex/water/PVC/air sample [Table 4.1, sample 7]

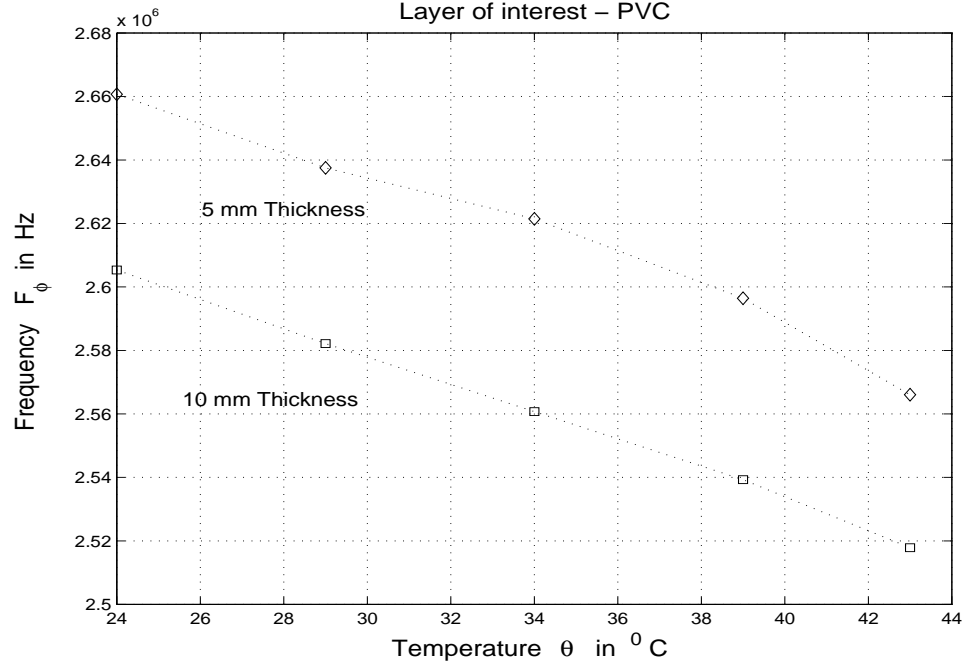


Figure 4.14: F_ϕ versus temperature θ for a water/PVC/water sample [Table 4.2, sample 1-2]

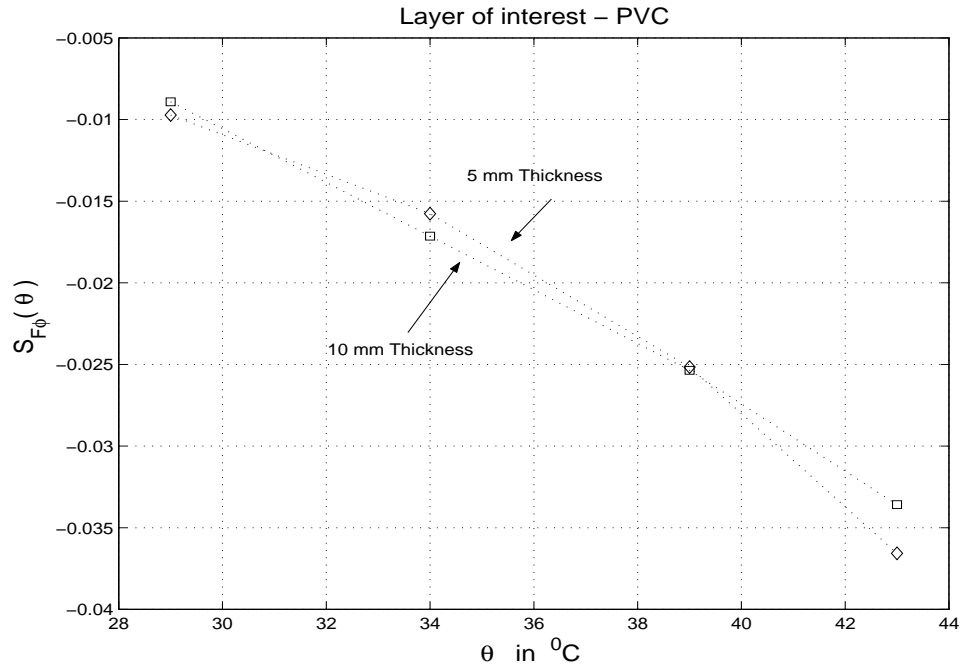


Figure 4.15: $S_{F_\phi}(\theta)$ versus temperature θ for a water/PVC/water sample [Table 4.2, sample 1-2]

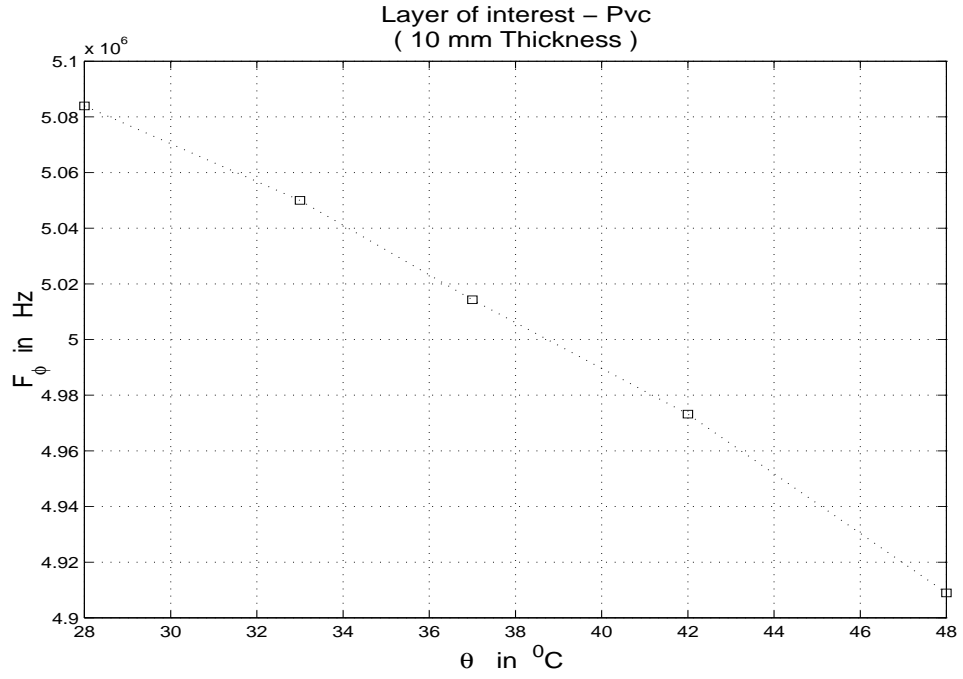


Figure 4.16: F_{ϕ} versus temperature θ for a multilayered water/PVC/water/Perspex/air sample [Table 4.2, sample 3]

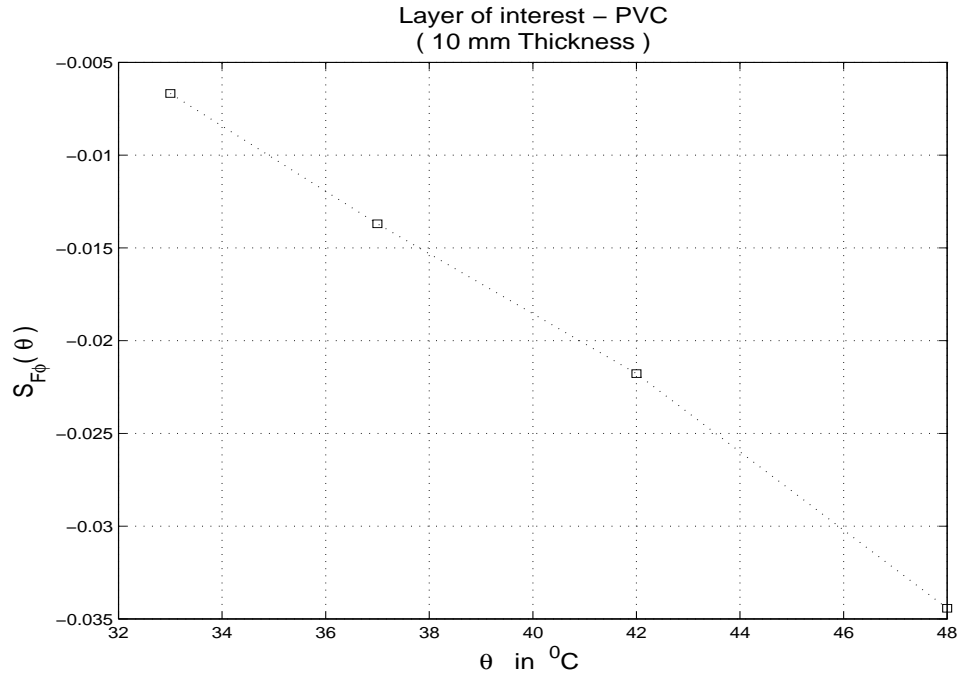


Figure 4.17: $S_{F_{\phi}}(\theta)$ versus temperature θ for a multilayered water/PVC/water/Perspex/air sample [Table 4.2, sample 3]

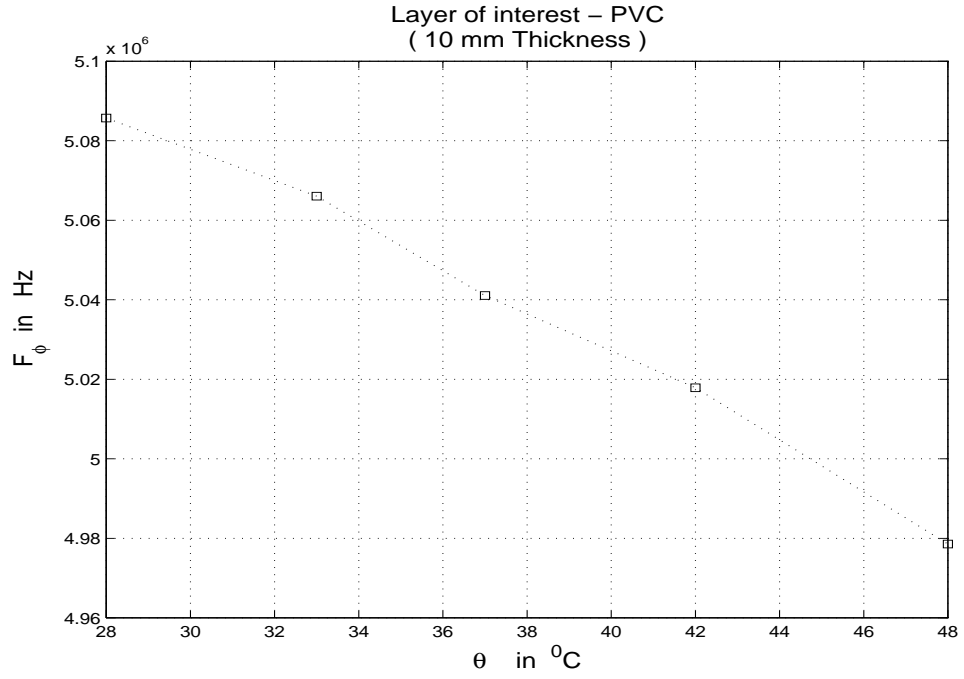


Figure 4.18: F_ϕ versus temperature θ for a multilayered water/Perspex/water/PVC/air sample [Table 4.2, sample 4]

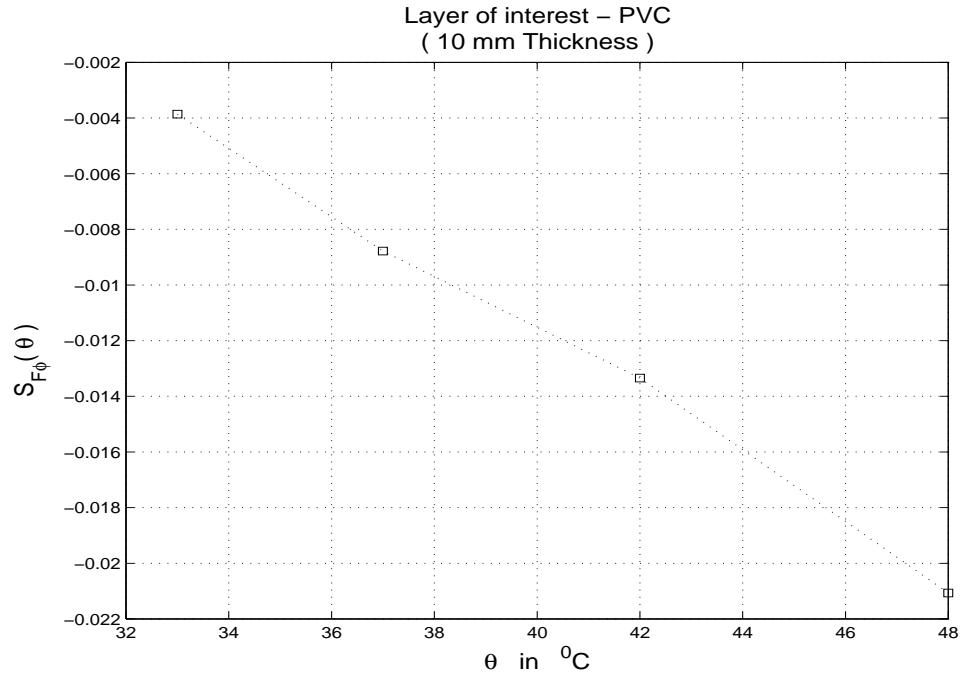


Figure 4.19: $S_{F_\phi}(\theta)$ versus temperature θ for a multilayered water/Perspex/water/PVC/air sample [Table 4.2, sample 4]

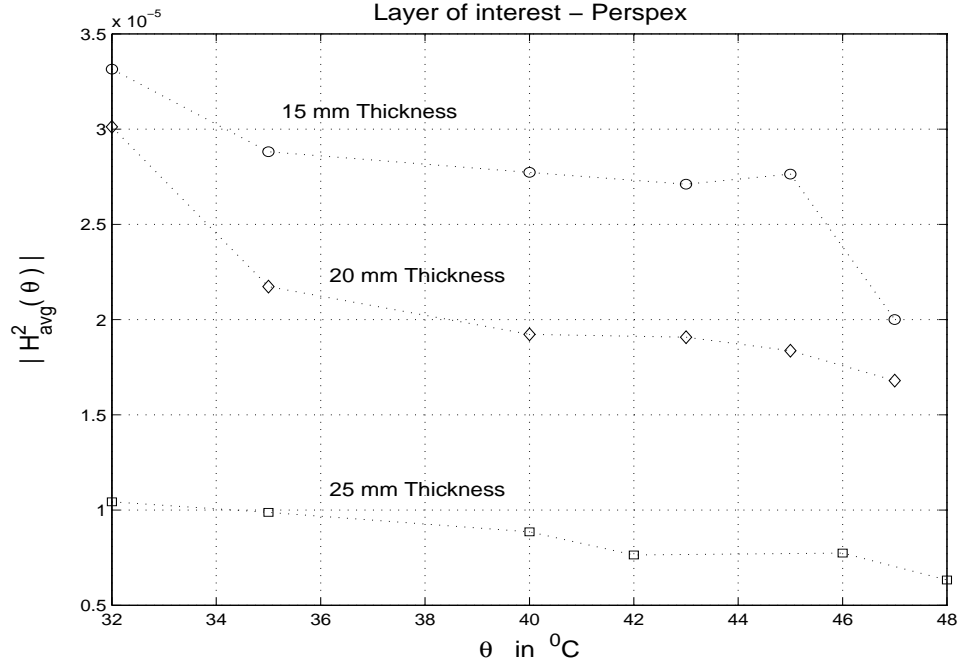


Figure 4.20: $|H^2_{avg}(\theta)|$ versus temperature θ for a water/Perspex/water sample [Table 4.1, sample 1-3]

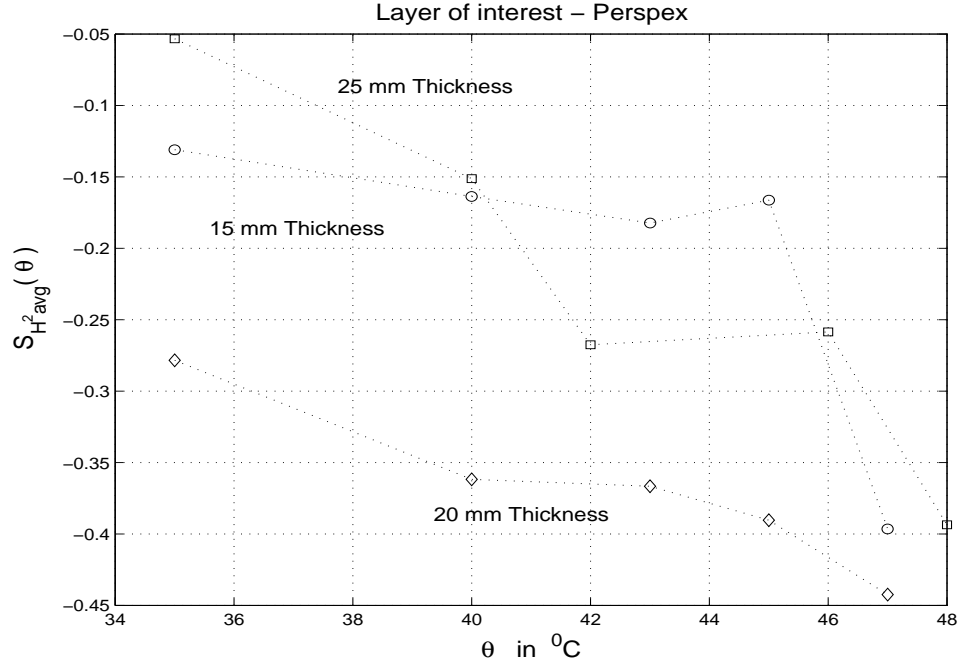


Figure 4.21: $S^2_{H^2_{avg}}(\theta)$ versus temperature θ for a water/Perspex/water sample [Table 4.1, sample 1-3]

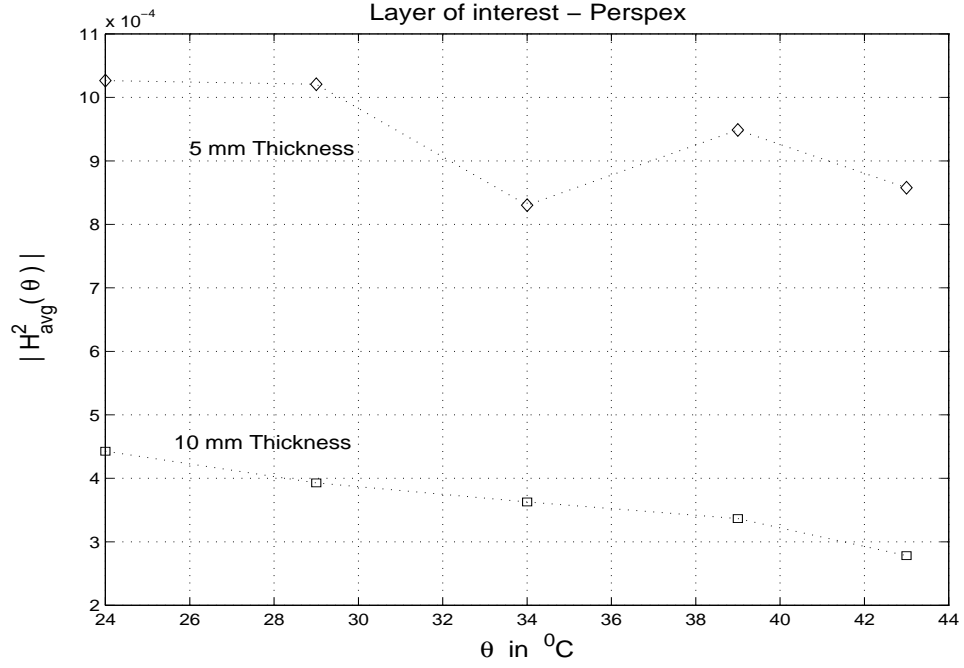


Figure 4.22: $|H_{avg}^2(\theta)|$ versus temperature θ for a water/Perspex/water sample [Table 4.1, sample 4-5]

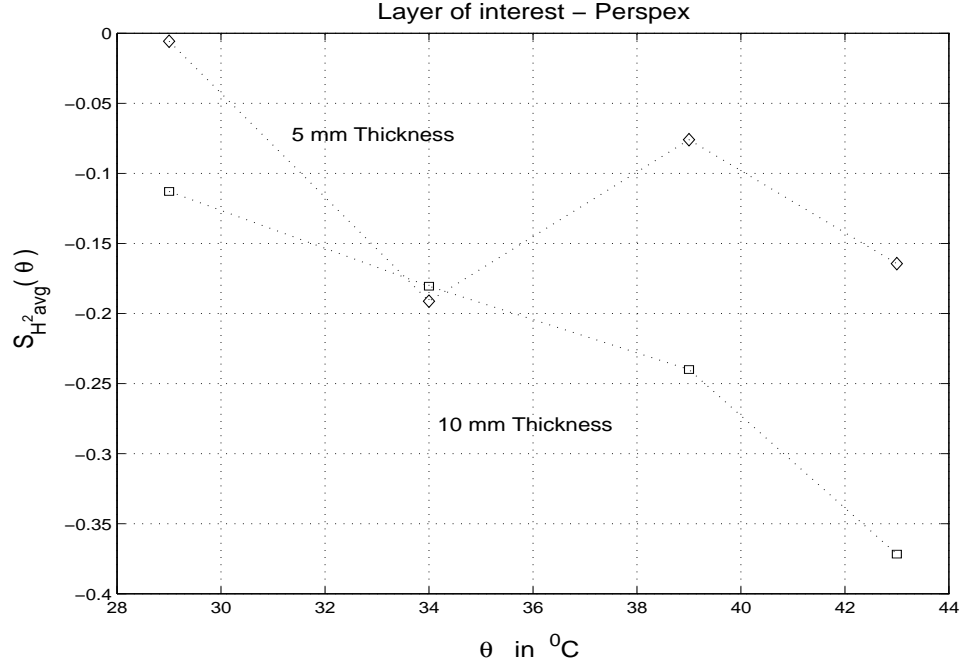


Figure 4.23: $S_{H_{avg}^2}(\theta)$ versus temperature θ for a water/Perspex/water sample [Table 4.1, sample 4-5]

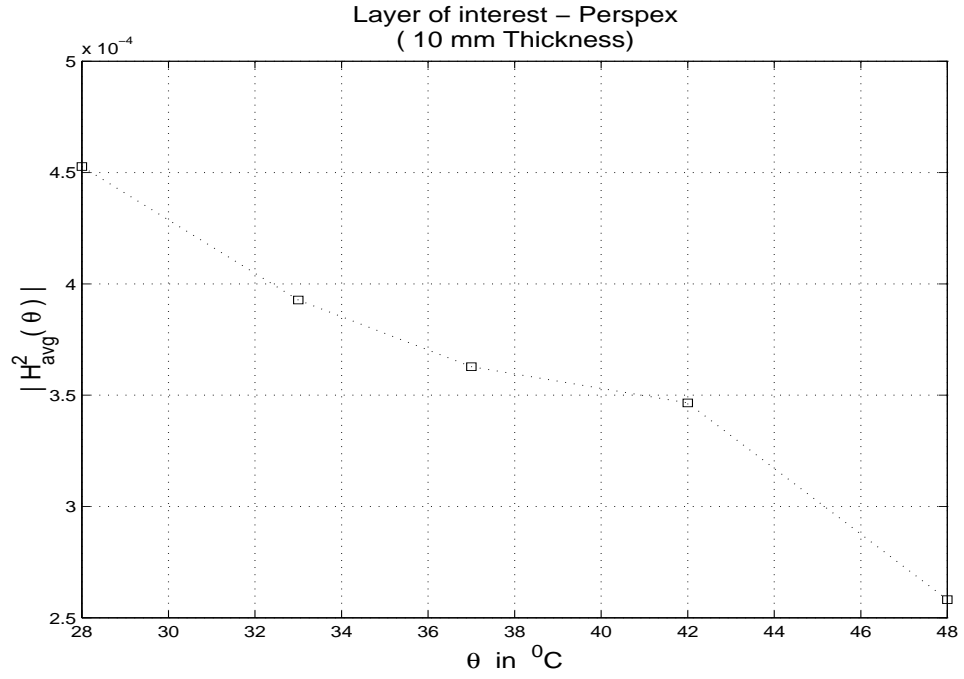


Figure 4.24: $|H_{avg}^2(\theta)|$ versus temperature θ for a multilayered water/PVC/water/Perspex/air sample [Table 4.1, sample 6]

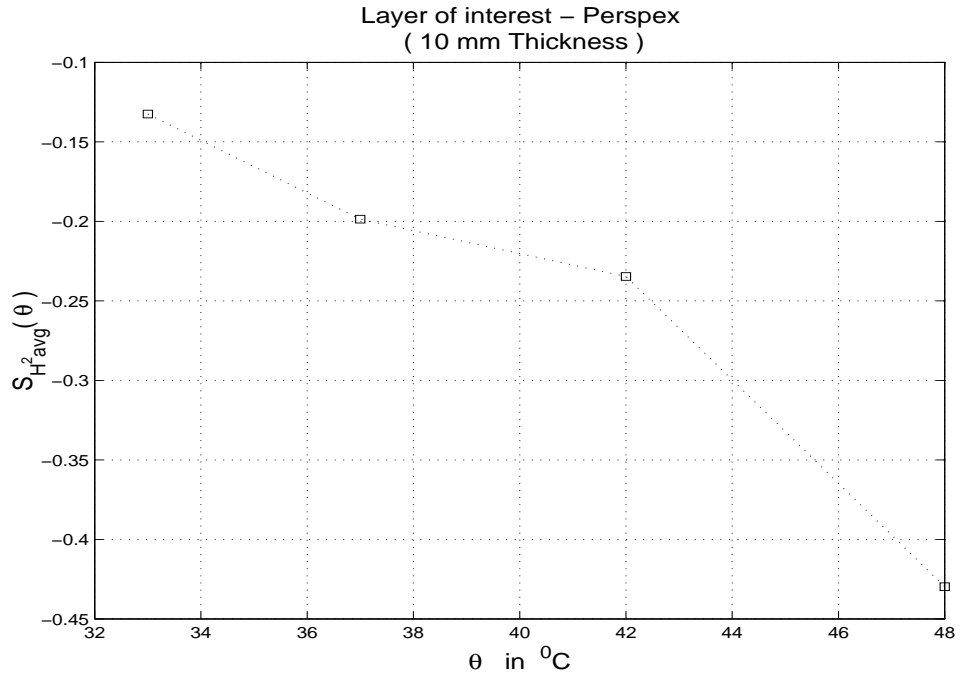


Figure 4.25: $S_{H^2}(\theta)$ versus temperature θ for a multilayered water/PVC/water/Perspex/air sample [Table 4.1, sample 6]

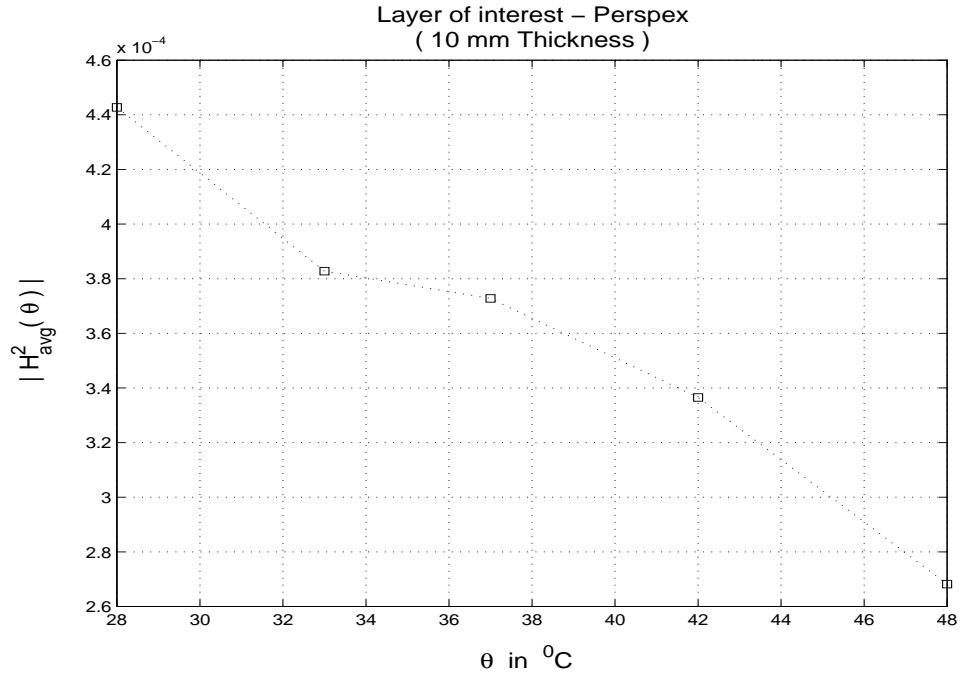


Figure 4.26: $|H^2_{avg}(\theta)|$ versus temperature θ for a multilayered water/Perspex/water/PVC/air sample [Table 4.1, sample 7]

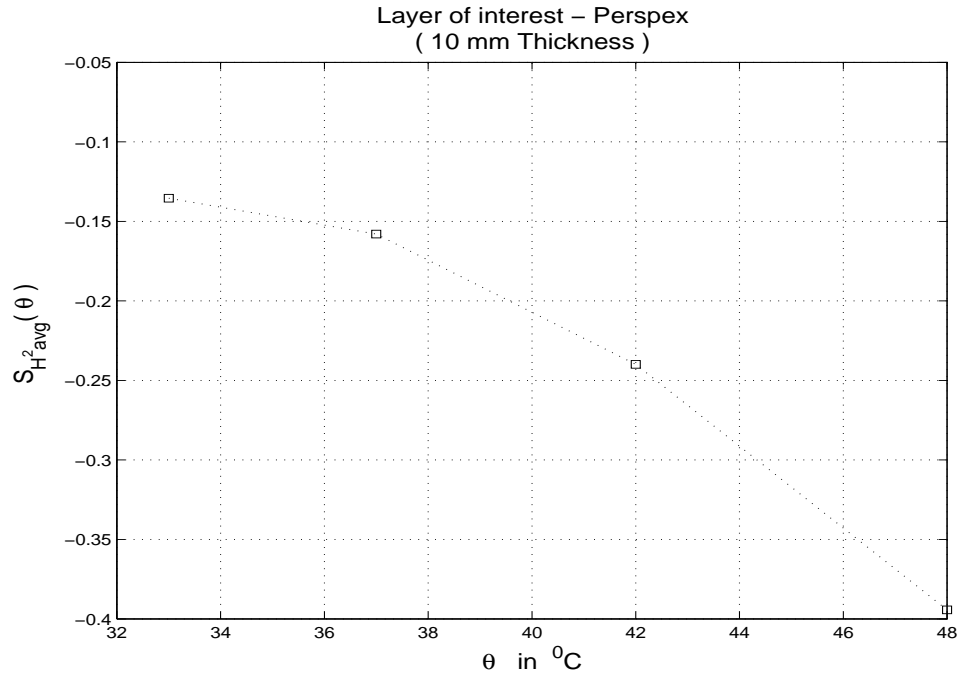


Figure 4.27: $S_{H^2_{avg}}(\theta)$ versus temperature θ for a multilayered water/Perspex/water/PVC/air sample [Table 4.1, sample 7]

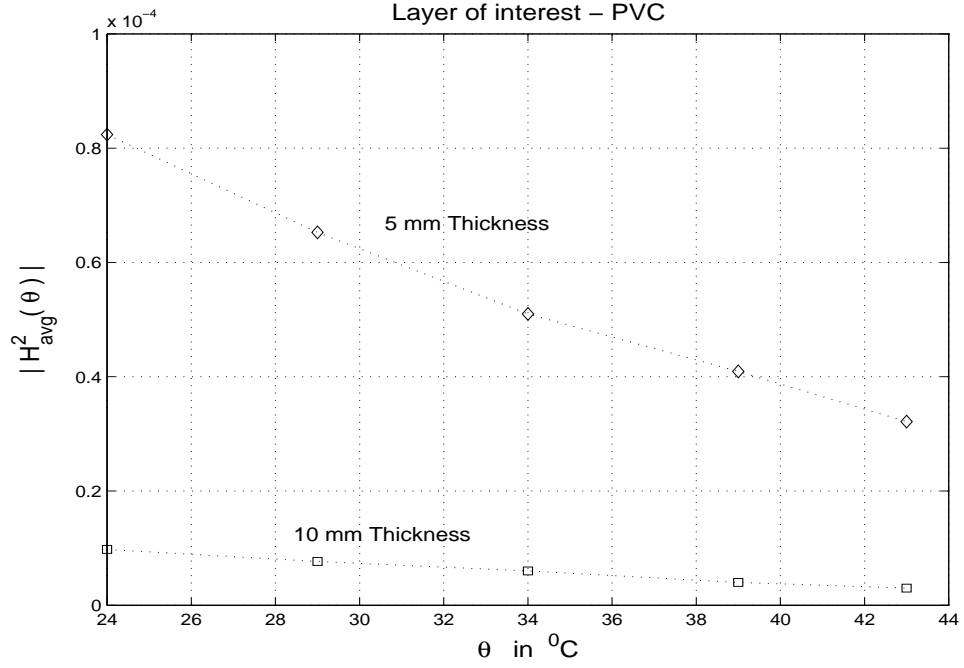


Figure 4.28: $|H^2_{avg}(\theta)|$ versus temperature θ for a water/PVC/water sample [Table 4.2, sample 1-2]

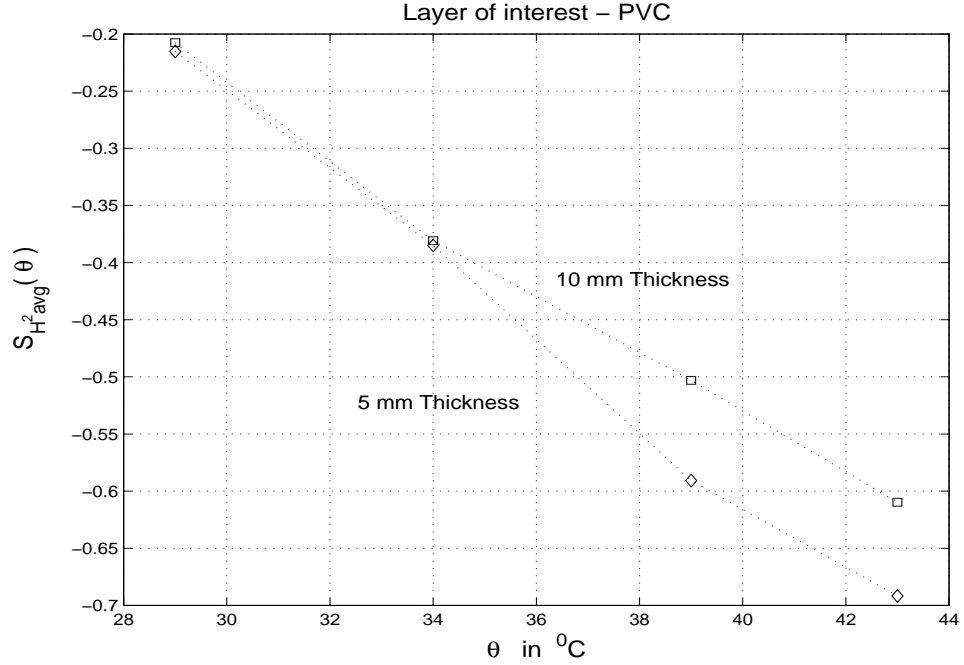


Figure 4.29: $S_{H^2_{avg}}(\theta)$ versus temperature θ for a water/PVC/water sample [Table 4.2, sample 1-2]

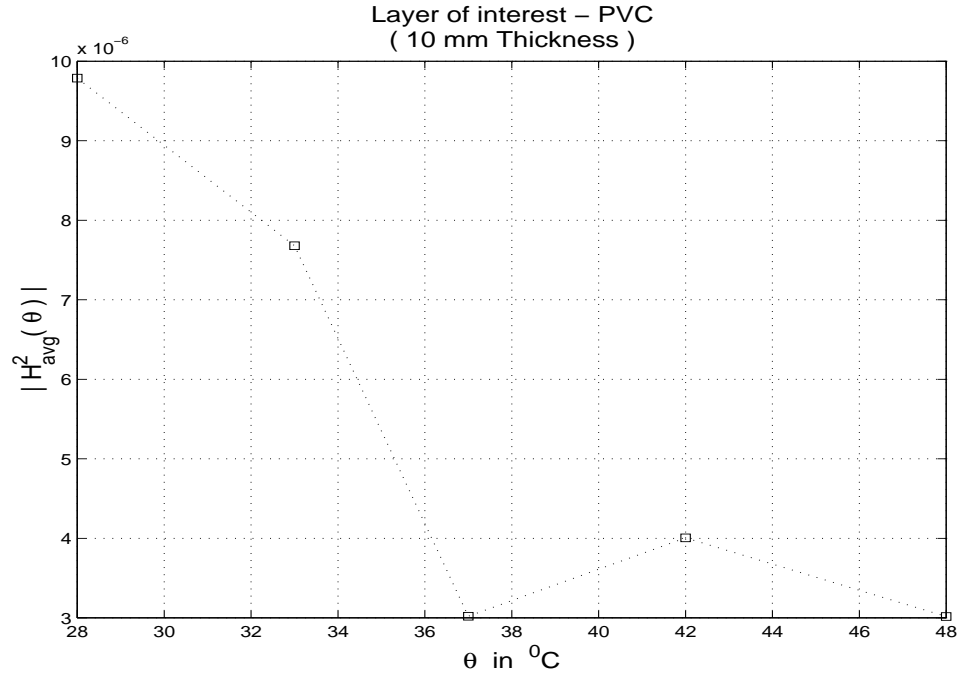


Figure 4.30: $|H_{avg}^2(\theta)|$ versus temperature θ for a multilayered water/PVC/water/Perspex/air sample [Table 4.2, sample 3]

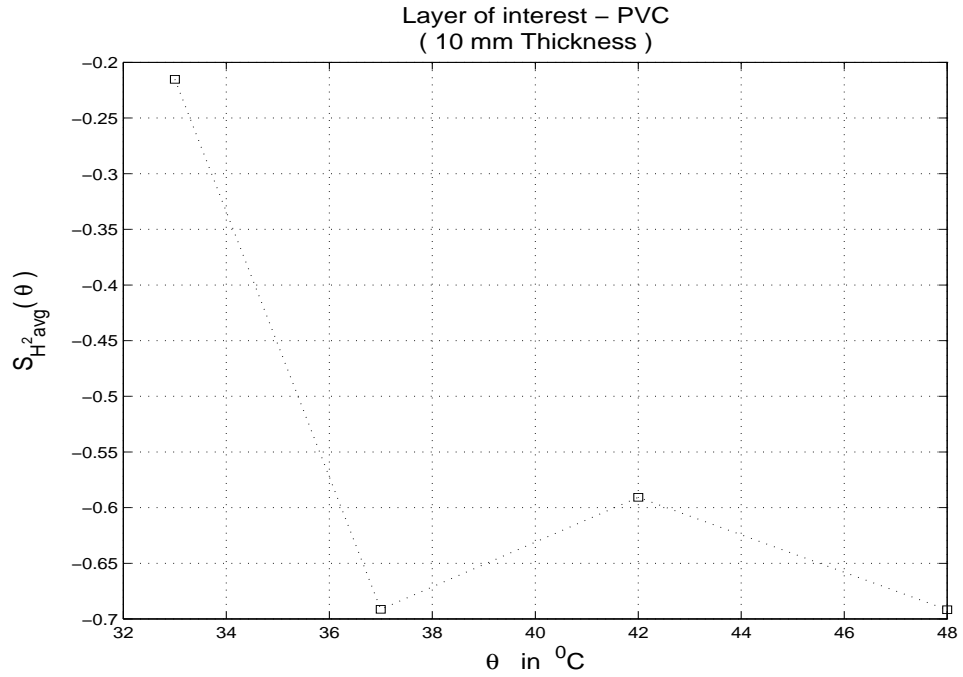


Figure 4.31: $S_{H_{avg}^2}(\theta)$ versus temperature θ for a multilayered water/PVC/water/Perspex/air sample [Table 4.2, sample 3]

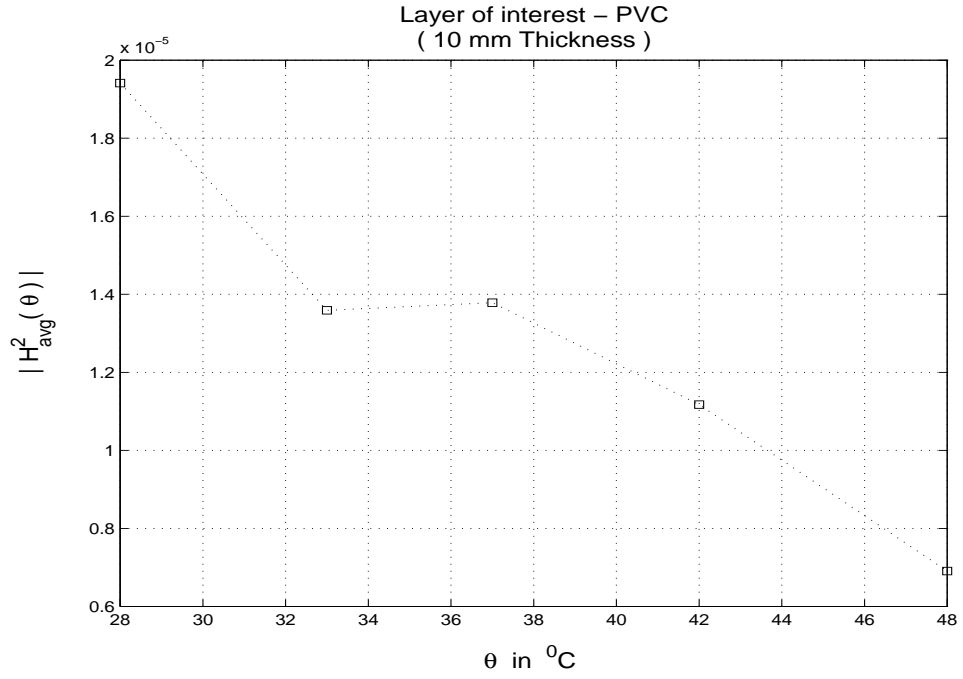


Figure 4.32: $|H^2_{avg}(\theta)|$ versus temperature θ for a multilayered water/Perspex/water/PVC/air sample [Table 4.2, sample 4]

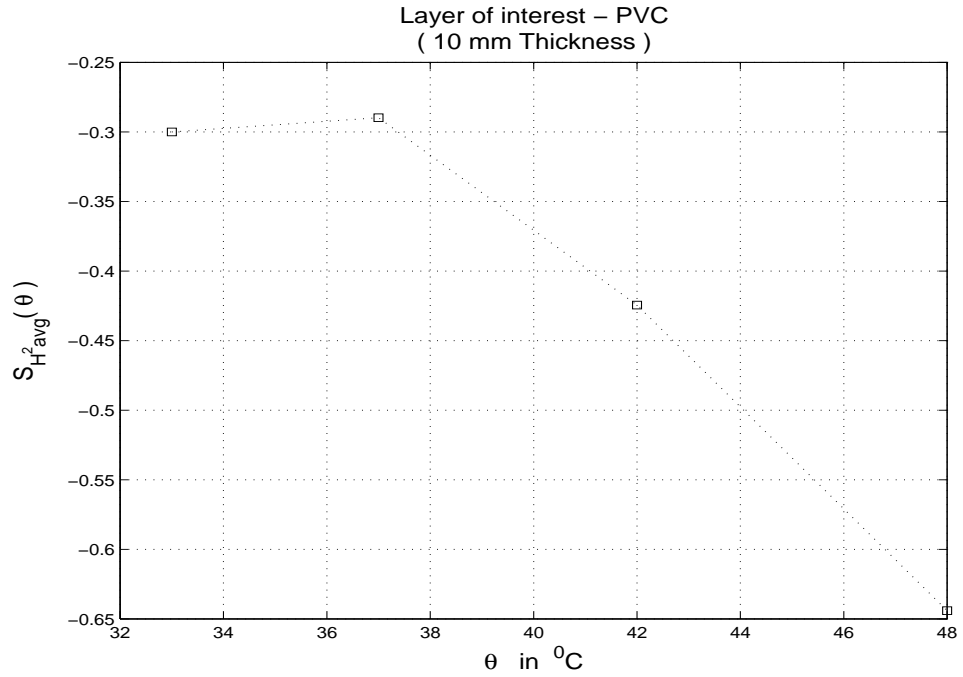


Figure 4.33: $S_{H^2_{avg}}(\theta)$ versus temperature θ for a multilayered water/Perspex/water/PVC/air sample [Table 4.2, sample 4]

Chapter 5

Summary and conclusions

Gadgil et al [3] developed techniques for estimation of temperature noninvasively. These techniques computed the transfer function of a material layer over a broad frequency band. Due to the presence of measurement noise, a large number of narrowband transducers were used to compute the pulse echo transfer function. The transfer function within the region of confidence for each transducer was computed. Portions of the response within the frequency band were retained. The response was truncated at the crossover points of the neighboring transducer characteristics. Using extrapolation and curve fitting techniques a magnitude response over a broad frequency band was computed. A number of techniques for estimating the attenuation coefficient from the transfer function were used. It was seen that attenuation coefficient, measured using the energy ratio method, exhibits a temperature sensitivity of 1.07 percent/ $^{\circ}\text{C}$ for Perspex and 1.49 percent/ $^{\circ}\text{C}$ for PVC.

As the technique developed by Gadgil et al [3] uses multiple narrowband transducers and involved digital processing, it is difficult to adapt it for an instrumentation system that could be used to measure temperature noninvasively.

In this project, a method to estimate the temperature of a material layer noninvasively using a single transducer was proposed. Instead of using attenuation coefficient derived from the transfer function, parameters that can be estimated from the transfer function over a narrow band were considered.

The transfer function of the material layer was computed using a single transducer and the phase and magnitude parts were analyzed. It was observed that with an increase in

temperature, the phase response shifts to the left in a monotonic fashion. The mean squared magnitude response of the transfer function also reduces monotonically with temperature. The frequency F_ϕ , in the range of confidence for the transducer, at which a phase shift of π occurs was taken as the parameter based on phase response for studying the effect of temperature variation. The temperature sensitivity of F_ϕ was found to be between 0.106-0.176 percent/ $^{\circ}\text{C}$ for Perspex and 0.172-0.184 percent/ $^{\circ}\text{C}$ for PVC. The temperature sensitivity values reported by Gadgil et al [3] for velocity are 0.13 percent/ $^{\circ}\text{C}$ and 0.15 percent/ $^{\circ}\text{C}$ respectively. Thus we can conclude that variation in F_ϕ is very closely related to variation in velocity.

Mean squared magnitude response, $H_{avg}^2(\theta)$ over a particular band was used as the magnitude response based parameter for studying the effect of temperature changes. In the temperature range of 35 - 45 $^{\circ}\text{C}$, the temperature sensitivity for layer thickness of 5 mm to 25 mm was found to be 1.13 - 2.62 percent/ $^{\circ}\text{C}$ for Perspex. For PVC, the temperature sensitivity for layer thicknesses of 5 mm and 10 mm was found to be in the range of 1.78 - 3.40 percent/ $^{\circ}\text{C}$

The temperature sensitivity of H_{avg}^2 is about an order of magnitude higher than that of F_ϕ . However the variation in F_ϕ was seen to be independent of the thickness of the material layer. Thus the phase response of the transfer function could be used to estimate the temperature of a material layer of unknown thickness. For a more meaningful comparison, precision of the two techniques needs to be established.

Suggestions for future work

In order to compare the phase response and the mean squared transfer function method, it is necessary to quantify the resolution with which the two parameters $H_{avg}^2(\theta)$ and $F_\phi(\theta)$ can be measured.

Experimental verification needs to be carried out with biological tissues. Finally, issues related to development of an instrument need to be considered.

References

- [1] T. Bowen, "Measurement of temperature dependence of velocity of ultrasound in soft tissues," *Ultrasonic Tissue Characterization*, NBS special publication 525, pp 57-62, 1979.
- [2] B.J. Davis and P.P. Lele, "An acoustic phase shift technique for noninvasive measurement of temperature changes in tissue," *Ultrasound symposium* vol. 2, pp 921-924, 1985.
- [3] C.P. Gadgil /Prof. S.C. Sahasrabudhe and Prof. T. Anjaneyulu (guides), "Study of influence of temperature on acoustic properties of materials for ultrasound thermometry," *PhD thesis*, Dept. of Electrical Engineering, IIT Bombay, 1993.
- [4] C.P. Gadgil, T. Anjaneyulu, and S.C. Sahasrabudhe, "Study of influence of temperature on acoustic properties of materials for ultrasound thermometry," *Proceedings of International Conference on Recent Advances in Biomedical Engineering*, Osmania University, Hyderabad, January 6-8, 1994.
- [5] A.C. Kak and A.K. Dines, "Signal processing of broadband pulsed ultrasound: Measurement of attenuation of soft biological tissues," *IEEE Trans. on Biomed. Engg.* vol.BME-25, pp.321-344, 1978.
- [6] M. Satio, W. Benjapolakul, and T. Shiina, "Basic discussion on noninvasive temperature measurement by reflected ultrasound," *JSUM Proceedings* pp. 665-666, 1986.

- [7] Ralph Seip, Emad S. Ebbini, "Noninvasive temperature estimation of tissue temperature response to heating fields using diagnostic ultrasound," *IEEE Trans. on Biomed. Engg.* vol.42, no.8, Aug. 1995.
- [8] John W. Strohbehn and Evan B. Douple, "Hyperthermia and cancer therapy: A review of biomedical engineering contributions and challenges," *IEEE Trans. on Biomed. Engg.* vol.31, no.12, Dec. 1984.
- [9] P.N.T. Wells, *Physical Principles of Ultrasonic Diagnosis*, London: Academic, 1977.